



LAWRENCE
LIVERMORE
NATIONAL
LABORATORY

Simulation of CO₂ Storage

W. McNabb, K. Myers

October 26, 2015

Disclaimer

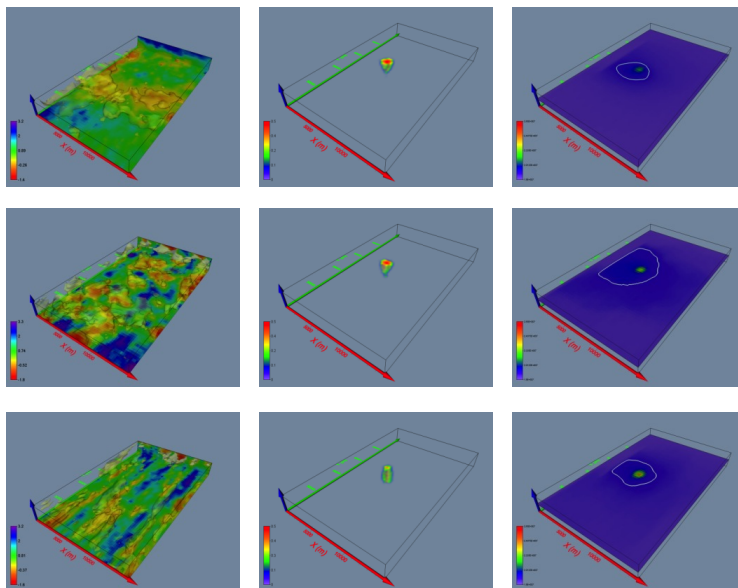
This document was prepared as an account of work sponsored by an agency of the United States government. Neither the United States government nor Lawrence Livermore National Security, LLC, nor any of their employees makes any warranty, expressed or implied, or assumes any legal liability or responsibility for the accuracy, completeness, or usefulness of any information, apparatus, product, or process disclosed, or represents that its use would not infringe privately owned rights. Reference herein to any specific commercial product, process, or service by trade name, trademark, manufacturer, or otherwise does not necessarily constitute or imply its endorsement, recommendation, or favoring by the United States government or Lawrence Livermore National Security, LLC. The views and opinions of authors expressed herein do not necessarily state or reflect those of the United States government or Lawrence Livermore National Security, LLC, and shall not be used for advertising or product endorsement purposes.

This work performed under the auspices of the U.S. Department of Energy by Lawrence Livermore National Laboratory under Contract DE-AC52-07NA27344.

Simulation of CO₂ Storage

CERC ACTC Subtask 6.4.a

12/4/2014



Prepared by LLNL under Contract DE-AC52-07NA27344.

This document was prepared as an account of work sponsored by an agency of the United States government. Neither the United States government nor Lawrence Livermore National Security, LLC, nor any of their employees makes any warranty, expressed or implied, or assumes any legal liability or responsibility for the accuracy, completeness, or usefulness of any information, apparatus, product, or process disclosed, or represents that its use would not infringe privately owned rights. Reference herein to any specific commercial product, process, or service by trade name, trademark, manufacturer, or otherwise does not necessarily constitute or imply its endorsement, recommendation, or favoring by the United States government or Lawrence Livermore National Security, LLC. The views and opinions of authors expressed herein do not necessarily state or reflect those of the United States government or Lawrence Livermore National Security, LLC, and shall not be used for advertising or product endorsement.

Contents

Contents	1
1 Executive Summary	2
2 Introduction	2
3 LLNL Research Team	3
4 Research Approach	3
5 Project Accomplishments	4
5.1 Accomplishments by Quarter	4
5.1.1 FY12 Q3 (April 1 – June 30, 2012)	4
5.1.2 FY12 Q4 (July 1 – September 30, 2012)	11
5.1.3 FY13 Q1 (October 1 – December 31, 2012)	20
5.1.4 FY13 Q2 (January 1 – March 31, 2013)	24
5.1.5 FY13 Q3 (April 1 – June 30, 2013)	24
5.2 Presentations	26
5.2.1 November 2012 Conference Poster	26
5.2.2 January 2013 Presentation: LLNL Input on Theme 6	30
5.3 Publications	44
5.4 US-China ACTC Research Overview	44
5.4.1 Theme 6 – Sequestration Capacity and Near-Term Opportunities	44
5.4.2 Accomplishments	44
5.4.3 Plans	45
5.5 CERC 2012-2013 Annual Report	45
5.5.1 CO2 Sequestration U.S. Research Team Leaders	45
5.5.2 Research Objective	45
5.5.3 Technical Approach	46
5.5.4 Recent Progress	47
5.5.5 Expected Outcomes	47

1 Executive Summary

This report is a compilation of Lawrence Livermore National Laboratory's (LLNL) accomplishments on CO₂ storage simulation and modeling research, performed for the US-China Clean Energy Research Center (CERC). Within the CERC project management structure, this work is referred to as Subtask 6.4.a Simulation and Modeling. The task falls under CERC's Advanced Coal Technology Consortium (ACTC) Research Theme 6—CO₂ Sequestration Capacity and Near-Term Opportunities. The goals of the task were to develop new CO₂ sequestration simulation approaches and tools, then apply them to CO₂ storage projects in the U.S. and China. Work on this task paused when funding was redirected to CERC's other efforts. Two sections of this report provide valuable snapshot of LLNL's progress when funding was curtailed: 1) Section 5.2.2 is a 14-page presentation written January 8, 2013; and 2) Section 5.1.3 is a progress report from the first quarter of Fiscal year 2013.

2 Introduction

The US-China Clean Energy Research Center (CERC) was established in November 2009 by Presidents Obama and Hu. CERC is made up of three consortia focused on building efficiency, clean vehicles and advanced coal technologies. The Advanced Coal Technology Consortium (ACTC) brings together many of the top scientists and leading companies in the power sector, who work together collaboratively to accelerate deployment of the most promising technologies and tackle some of the most pressing issues in making coal plants more efficient and environmentally friendly.

Reducing carbon emissions in the power sector is a central goal for both US and Chinese decision makers and industrial leaders, since, worldwide, coal power plants produce nearly 40% of greenhouse gases. In order to deeply reduce their greenhouse gas emissions, many utilities are considering carbon capture, utilization, and sequestration (CCUS). CCUS can enable the current fossil fuel infrastructure to be utilized while non-fossil fuel based energy supplies evolve to replace fossil fuels. One aspect of CCUS is addressed under ACTC's Research Theme 6—CO₂ Sequestration Capacity and Near-Term Opportunities.

Lawrence Livermore National Laboratory (LLNL) performed research on one subtask of Theme 6, referred to as Subtask 6.4.a – Simulation and Modeling. The goals of LLNL's CO₂ storage simulation and modeling research were to develop new CO₂ sequestration simulation approaches and tools, then apply them to CO₂ storage projects in the U.S. and China. Work on this task paused when funding was redirected to CERC's other efforts. This report presents the progress made on this subtask when funding was curtailed.

3 LLNL Research Team

The following people worked on the subtask.

Name	Role	Status as of November 2014
Walt McNab	Theme Lead	No longer at LLNL
Jeff Wagoner	Geologic Modeling, EarthVision	At LLNL
Mingjie Chen	Geologic Modeling, EarthVision Cellular Gridder, NUFT	No longer at LLNL, but his computer and files are accessible to two other modelers: Jeff Wagoner and Yue Hao.

4 Research Approach

Under the simulation task, advanced subsurface modeling tools and approaches were applied to CO₂ storage projects in the U.S. and China and new simulation approaches and tools were being developed to address the issue of parameter uncertainty. Modeling tools were used to assess a number of key performance questions as well as to provide quantitative insights that feed into risk characterization, including:

- Quantification of injection mass fluxes and pressures
- Mapping of potential fluid pressure and CO₂ saturation distributions throughout the target reservoir
- CO₂ storage capacity
- Evaluation of leakage pathways for injected CO₂
- Assessment of effective stress on nearby faults
- Gauging the induced seismicity potential
- Quantifying CCS efficacy when used in conjunction with enhanced oil recovery

U.S. and Chinese scientists involved in the subsurface simulation task met in Wuhan, China in March 2012 to develop a detailed work plan and schedule deliverables. Those were summarized in a set of ten-point plans, submitted separately to DOE. In summary, the overarching goals of the simulation task was to develop templates and protocols for demonstration project evaluation, model development, and larger scale injection predictions; assemble a catalog of models and techniques and apply to site data sets, as warranted; compare results and summarize general findings; understand similarities and differences of CCS and CCUS risk assessment methods, needs, and goals between the U.S. and Chinese teams; identify key sites and specific hazards (including economic issues); develop abstractions of subsurface simulations to inform risk calculations; and calculate risk profiles for selected projects and use demonstration scale data to predict larger scale system behavior. These goals were to be addressed using sites in both the U.S. in China as example application, including:

- Ordos Basin, China: saline aquifer geologic storage in Paleozoic units
- Wyoming, USA: saline aquifer geologic storage in the Madison and/or Weber Formations

- Illinois Basin, USA: Saline aquifer geologic storage in the Wabash Valley in the Mount Simon Formation. Of particular interest to the simulation task is the planned injection of CO₂ at the Gibson-3 coal-fired power plant unit in Indiana, where a partnership between Duke Energy and China Huaneng Group to collaborate on CO₂ capture is in place. The simulation task will focus particular effort on this site, since clear synergies exist between the CO₂ capture and storage efforts (e.g., determining the optimal CO₂ flux for capture and subsequent storage) and the interests of the Chinese and U.S. partners directly converge.

5 Project Accomplishments

The following resources were used to document the progress of this project: quarterly progress reports, presentations, and publications. Applicable highlights from each are presented below.

5.1 Accomplishments by Quarter

Accomplishments on this project were described in progress reports submitted to CERC ACTC from the third quarter of Fiscal Year 2012 (FY12/Q3), to FY13/Q3. Below are excerpts from the reports.

5.1.1 FY12 Q3 (April 1 – June 30, 2012)

During the past quarter, LLNL's modeling efforts under Subtask 6.4 have focused on three areas: (1) CO₂ injection at the Gibson-3 site in southwest Indiana, one of the sites agreed upon by the U.S and Chinese teams, (2) consideration of CO₂ injection-enhanced oil recovery in CCS simulations, and (3) development of modeling approaches to address enhanced coal bed methane, one of the four research thrusts developed by the U.S. and Chinese teams at the March 2012 joint meeting in Wuhan, China. Progress in each area is summarized below.

5.1.1.1 *Simulation of CO₂ Injection at the Gibson-3 Site, Illinois Basin, U.S.A.*

The current data sets employed in the Gibson-3 modeling effort include:

- A preliminary geologic model
- Limited porosity and permeability data identified; data collection effort currently focusing on including additional data sets
- Some laboratory relative permeability data for samples from Knox Formation
- Stress field analyses available from the Knox carbonate section from the Mountaineer site
- Geomechanical properties to be inferred from waveform sonic data (pending)
- Regional brine chemistry data

To date, the simulation task has involved initial screening level modeling to bound pressure distributions in the target injection reservoir, subject to assumptions concerning formation permeability, structure, and relative permeability values gleaned from available field and laboratory data. Modeling of CO₂ injection is particularly focused on quantifying the potential for induced seismicity along two fault segments extending through the target Knox formation some 3-4 km west of the Gibson-3 coal-fired power plant. Because the permeability structure in the target reservoir at Gibson-3 is not well characterized, different modeling approaches are being used to assess the uncertainties associated with model predictions. This includes comparison of the results of a conventional finite difference simulator,

applied to a stochastically generated permeability field based on similar carbonate reservoir properties, with those of a rapid semi-analytical screening model (Figures 6.4.1 – 6.4.4; Table 6.4.1). A manuscript describing the semi-analytical screening model has been submitted for publication in *Transport and Porous Media*, while an abstract describing the comparison between the finite-difference and semi-analytical modeling approaches has been accepted for presentation at the Greenhouse Gas Technologies conference (GHGT-11) in Kyoto, Japan in November 2012.

An additional modeling for the Gibson-3 site entails the application of a multi-parameter model emulator to function as a computationally efficient proxy for LLNL's multicomponent, multiphase NUFT flow and transport model. This effort involves developing a multidimensional objective response surface, conditioned to the NUFT pressure and CO₂ distribution output for a series of runs reflecting different assumptions regarding permeability distributions within the reservoir and surrounding units. The resulting response surface is then used to quantify model sensitivity to parameter values with high fidelity. These results will be presented in the next quarterly report.

5.1.1.2 Simulation of CO₂ Injection Coupled with Enhanced Oil Recovery (CCS-EOR)

A second component of the simulation task undertaken in the past quarter has entailed a numerical modeling study of CCS deployment in conjunction with enhanced oil recovery (EOR) in depleted oil reservoirs with low oil saturation which would otherwise not be economically favorable to exploit. The objective of the modeling is to compare the amount of additional oil recovered to the mass of CO₂ injected, under a range of reservoir and unsaturated flow conditions, to gauge the net benefit of the CCS operation. Application of EOR with supercritical CO₂ to very-low oil saturation environments across particularly on a reservoir scale, has not received extensive study, particularly in the context of comparing enhanced oil extraction against the mass of carbon stored. This knowledge gap for CCS-EOR deployment is being addressed through a systematic numerical modeling study which will address the oil-recovery and carbon balance metrics in the context of heterogeneous permeability fields associated with both carbonate and siliceous clastic reservoirs, published multiphase relative permeability and capillary relationships, initial residual oil saturations as affected by rock and fluid properties as well as past extraction, and different operational modes of injection. Modeling is employing LLNL's NUFT multiphase flow model to consider ranges of possible scenarios, allowing a quantitative comparison of oil extraction enhancement against stored CO₂ volume as a function of physical, chemical, and operational parameters (Figures 6.4.5 – 6.4.9).

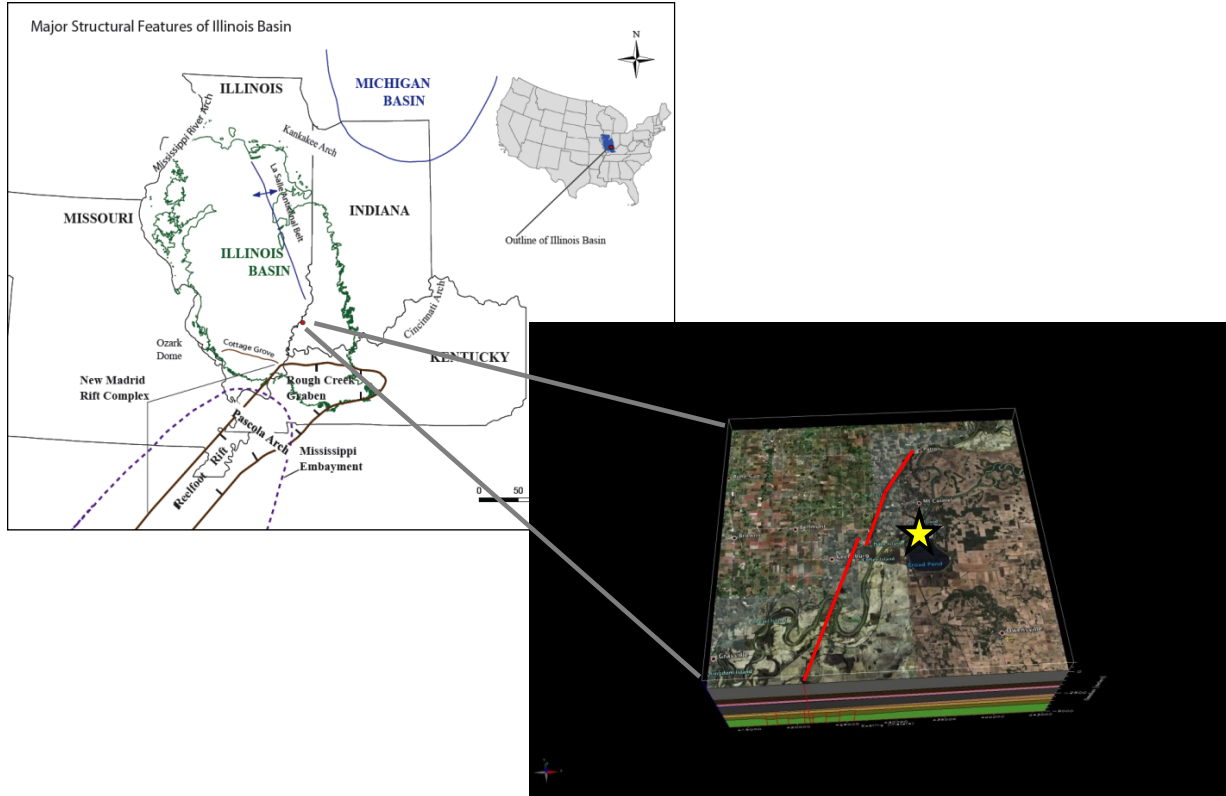


Figure 6.4.1. Gibson-3 site location in the Illinois Basin, southwest Indiana.

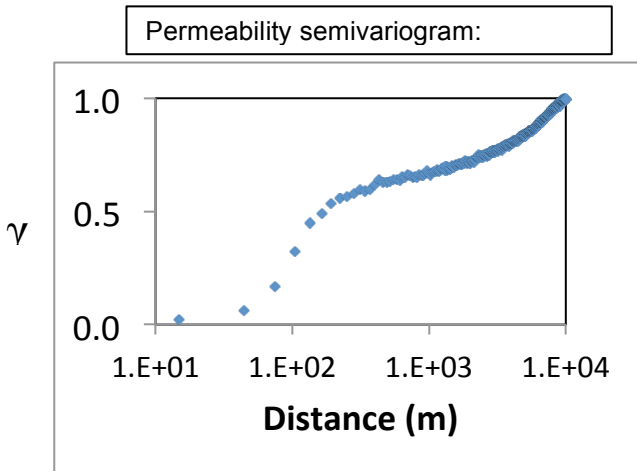
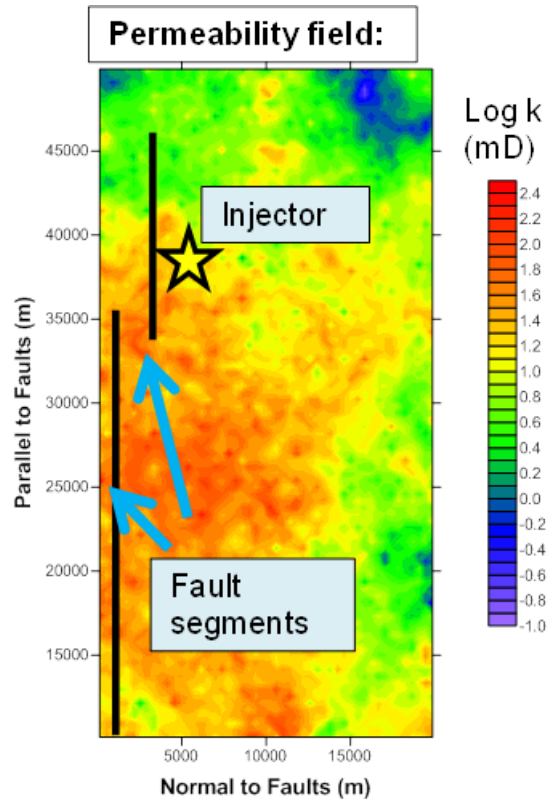
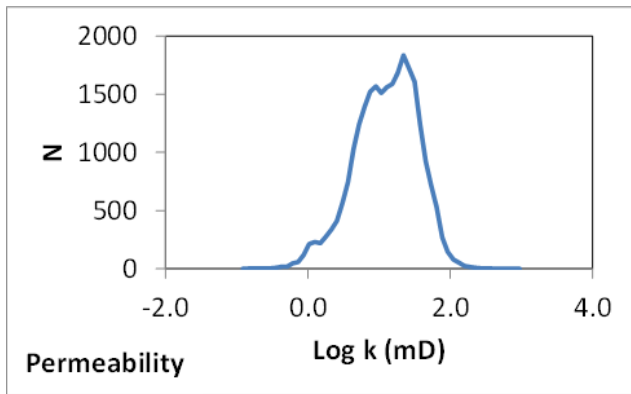


Figure 6.4.2. Permeability and porosity distributions are based on a stochastic realization using property distributions from the Weyburn-Midale carbonate reservoir in Canada, an analogue formation.

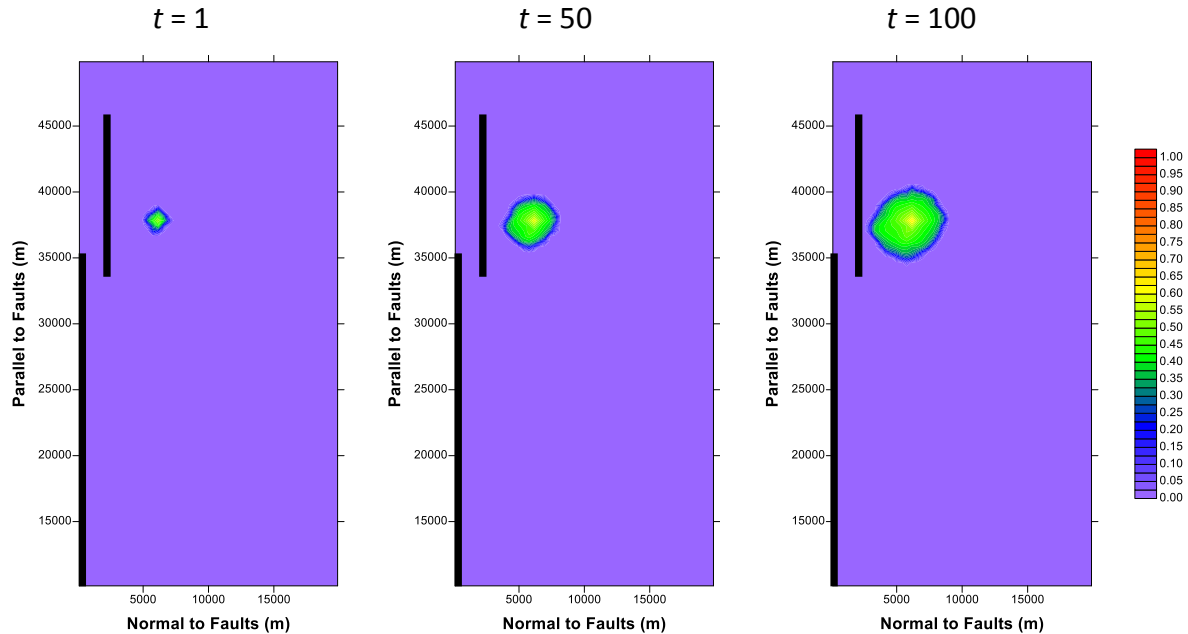


Figure 6.4.3. Distribution of CO₂ at the top of a putative injection horizon within the Knox Formation as a function of time; Q = 1 MT CO₂/yr; depth = 1,800 m; target zone thickness = 200 m; porosity ~ 0.1 (variable).

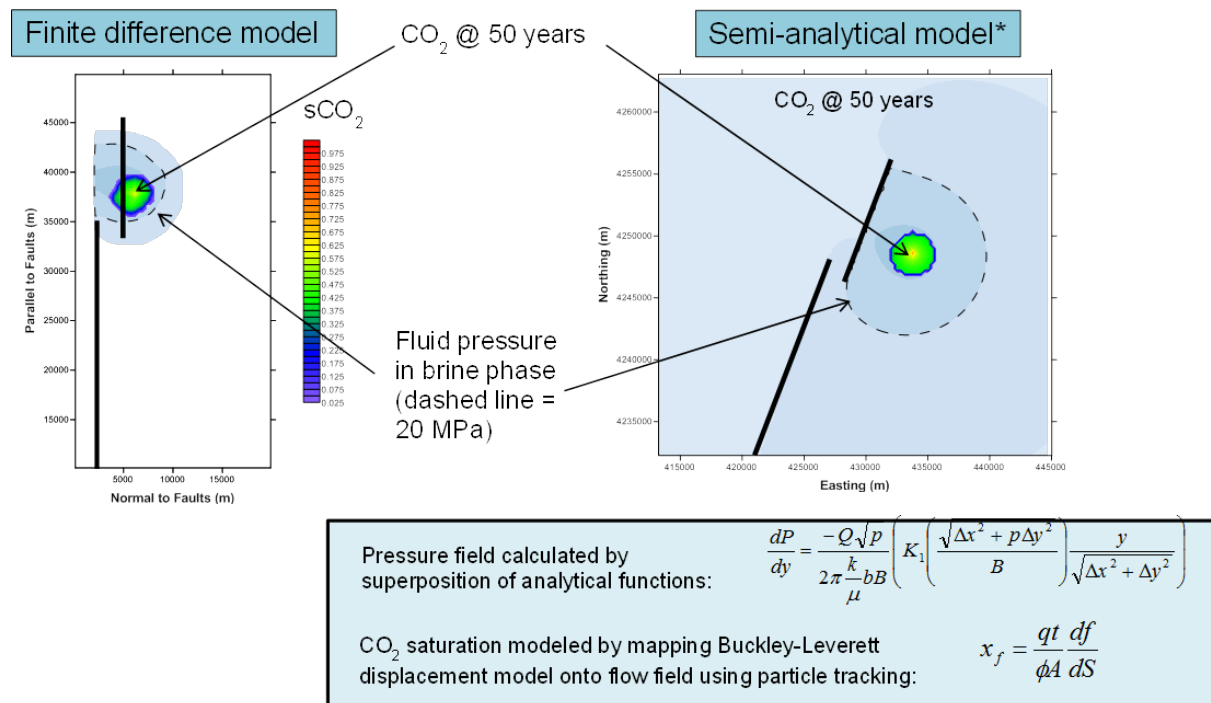


Figure 6.4.4. Comparison of simulate fluid pressure distributions predicted by the finite-difference model (with permeability and porosity heterogeneities) and the semi-analytical screening model.

	k_x (mD)	k_y (mD)	Anisotropy Direction (°)	Reservoir Thickness (m)	k_{caprock} (μD)	Caprock Thickness (m)	Max. P @ Fault (bar)
MC Run 1	6.6	3.0	27.3	276	<0.5	968	281.8
MC Run 2	6.6	5.2	40.0	417	<0.5	884	231.6
MC Run 3	75.3	34.5	27.7	268	1.1	558	191.3
MC Run 4	17.4	10.4	15.7	302	<0.5	546	207.9
MC Run 5	7.3	4.1	30.9	104	<0.5	541	333.5
MC Run 6	66.9	28.1	39.4	254	<0.5	823	193.8
MC Run 7	52.5	11.0	11.6	549	0.7	842	192.7
MC Run 8	17.5	5.1	22.6	147	<0.5	752	267.9
MC Run 9	17.3	16.3	7.8	541	<0.5	824	199.7
MC Run 10	26.1	14.7	6.7	110	<0.5	849	243.0
Finite difference baseline	Variable	Variable	-	200	-	-	205.3

Table 6.4.1. Example multi-run output from the semi-analytical screening model which allows for rapid evaluation of fluid pressures and CO₂ distributions for sparsely characterized sites. This capability enables Monte Carlo simulations that can easily address thousands of realizations, yielding distributions of performance criteria metrics (e.g. fluid pressures along faults) as a function of parameter values.

Figure 6.4.5. Heterogeneous permeability field for coupled CCS-EOR simulation, with a horizontal injection well indicated by red prism (bottom) and production well (constant fluid pressure) indicated at top. Reservoir thickness is 200 m; horizontal scale is 4 km x 4 km.

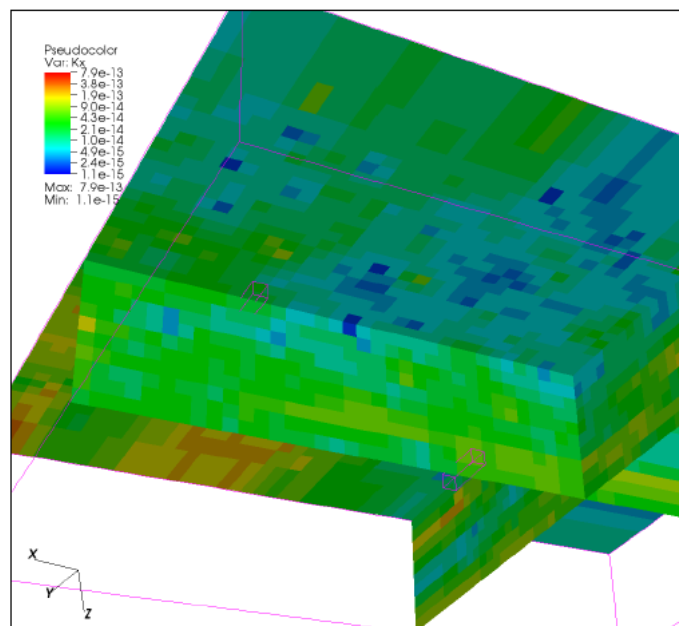


Figure 6.4.6. Distribution of CO₂ saturation in CCS-EOR simulation after 20 years of injection at approximately 1 MT CO₂/yr.

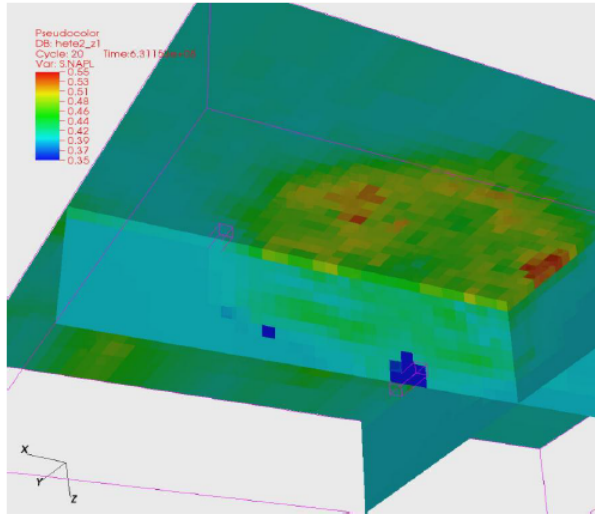
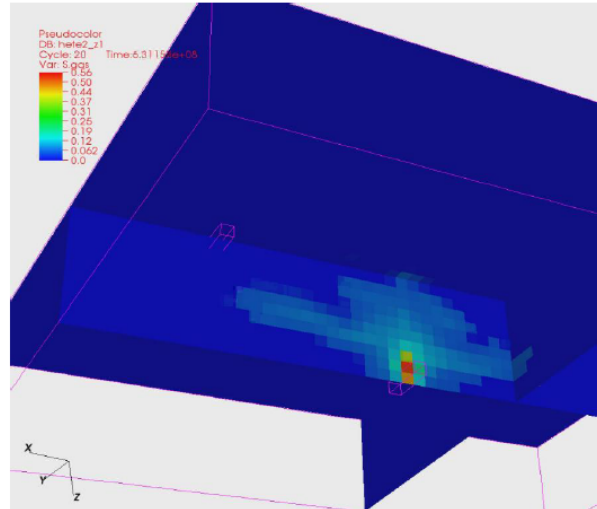


Figure 6.4.7. Distribution of oil phase saturation in CCS-EOR simulation after 20 years of injection at approximately 1 MT CO₂/yr.

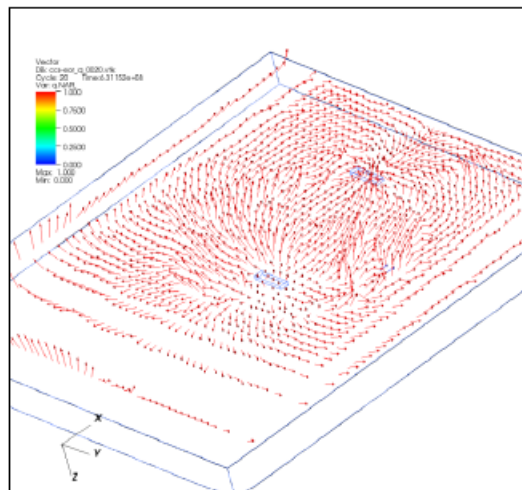
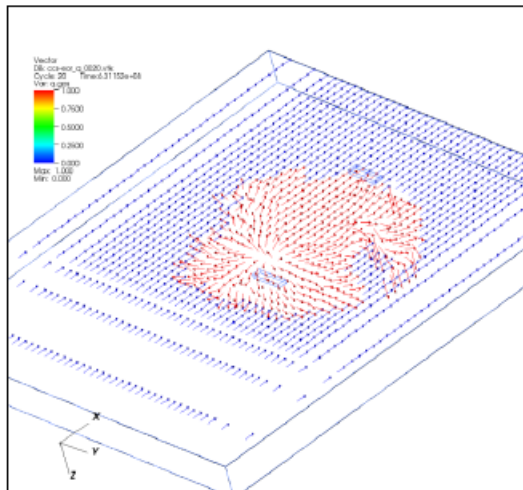


Figure 6.4.8. Three-dimensional fluid flow fields associated with CO₂ (left) and oil (right) after 20 years of injection into a heterogeneous reservoir. $S_o = 0.36$.

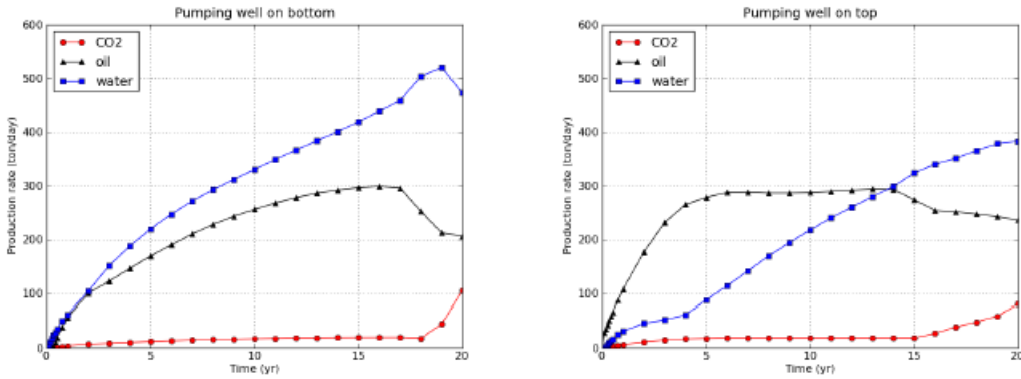


Figure 6.4.9. Mass removal histories associated with CCS-EOR for a production well placed at the bottom of the formation (left) and the top of the formation (right), indicating the influence of buoyancy in determining the optimal placement of the production well. Initial oil saturation $S_o = 0.36$.

5.1.2 FY12 Q4 (July 1 – September 30, 2012)

During the past quarter, LLNL’s modeling efforts under Subtask 6.4a have continued to focus on modeling methodology development, specifically addressing the need for computationally efficient screening-model approaches that are applicable to sites with limited geologic characterization. We have completed development of a semi-analytical modeling tool for CO2 injection and storage in idealized systems and are currently using a multi-process model emulator to assess CO2 storage in complex environments in a computationally expedient manner. Both approaches have been applied to the Gibson-3 site in Indiana, one of the three sites agreed to by the U.S. and Chinese CERC partners. With completion of this work, we are positioned to test the new modeling approaches on the other two sites.

5.1.2.1 Screening Model Overview

Multiphase flow through porous media encompasses a range of phenomena, including partially-miscible displacement of one fluid phase by another, capillary forces, mechanical deformation, inter-phase dissolution, and reactive chemistry involving the solid matrix. High-fidelity simulation of a full suite of processes requires complex, coupled numerical models which are demanding in terms of both computational burden and input data requirements. However, the distributions of key parameters such as permeability are often poorly resolved at the aquifer or reservoir scale. Therefore, it may be expedient in many instances to employ more simplified but highly computationally efficient screening models which approximate saturation and pressure distributions to a level which may suffice for practical engineering applications.

The simplest conceptual model for multiphase flow is immiscible fluid displacement in the absence of capillary pressure, as described by the Buckley-Leverett equation:

$$\frac{\partial S}{\partial t} = \frac{Q}{\phi A} \frac{df}{dS} \frac{\partial S}{\partial x} \tag{1}$$

where S is fluid saturation, ϕ the porosity, A the cross sectional area, and f the fluid flow fraction of a non-aqueous phase displacing water,

$$f = \frac{1}{1 + \frac{k_{r,na}\mu_w}{k_{r,w}\mu_{na}}} \quad (2)$$

The parameters $k_{r,w}$, $k_{r,na}$, μ_w , and μ_{na} correspond to the relative permeabilities and viscosities of the water and non-aqueous phases, respectively. Equation (1) can be solved analytically for the limiting one-dimensional case when capillary forces are neglected, although a variety of solutions for less restrictive assumptions have been developed.

In this study, a screening tool for CO₂ storage problems is developed which maps the Buckley- Leverett solution, via particle tracking, to a fluid flow field determined by an analytic element model. A set of heuristic rules are used to adjust fluid pressures as a result of changing fluid saturations. The analytic element approach allows the effects of simple flow heterogeneities to be addressed through the use of integrated line sources and doublets to represent horizontal injectors and impermeable faults. Simplifying assumptions include a two-dimensional reservoir of uniform thickness and anisotropic permeability, a leaky confining layer or cap rock, and steady-state, incompressible, fixed-viscosity fluid injection or withdrawal. Buoyancy and capillary forces are neglected.

5.1.2.2 Flow Model Development

The analytic element concept for simulating flow in porous media bridges gaps in both model complexity and simulation capability between simple analytical models and numerical simulators. Analytic elements representing lines sources, sinks, and other flow-controlling features are discretized, as opposed to the discretization of the entire flow domain for numerical finite difference or finite element models. In this current study, we employ a modified analytic element methodology which allows for a leaky confining layer, based on the superposition of pressure-influencing terms. A basic element is a single point source, for which the impact on reservoir fluid pressure is given by De Glee 1930; 1951:

$$\Delta P = \frac{Q\sqrt{p}}{2\pi\frac{k_x b}{\mu}} K_0 \left(\sqrt{\Delta x^2 + p\Delta y^2} \sqrt{\frac{k_c}{k b b_c}} \right); \quad (3)$$

where Q is the volumetric injection rate, k_x the reservoir permeability along the principal coordinate axis, k_c the cap rock permeability, μ the fluid viscosity, b the reservoir thickness, b_c the cap rock thickness, Δx and Δy are the distances along the respective axes between the element location and the monitor point, and $p = k_x/k_y$. The function K_0 corresponds to the modified Bessel function of the second kind and zero order. Numerical integration using Gaussian quadrature or similar scheme along a line segment within the reservoir yields an expression for the pressure impact of a horizontal injection well.

A second type of finite-length element is a flow doublet, which serves as a basis for quantifying flow around low-permeability features such as fault segments within the reservoir. The flow field associated

with a hypothetical point doublet is proportional to $\cos \theta/r$, where θ refers to the angle formed between the element, the monitoring point, and the x -axis. For a finite-length element extending from $x = x_0$ to $x = x_f$,

$$\Delta P = \frac{Q\sqrt{p}}{2\pi \frac{k}{b} \mu} \int_{x=x_0}^{x=x_f} \frac{\Delta x dx}{\sqrt{\Delta x^2 + p\Delta y^2}} \quad (4)$$

Pressure gradients and hence fluid velocities corresponding to Equations 3 and 4 are given by the derivatives of these equations with respect to x and y . The reservoir fluid pressure and fluid velocity distributions are then calculated by superimposing the perturbations associated with each element through a combination of analytical and numerical integration. For problems with initially unknown fluxes (e.g, doublet line elements, fixed-pressure injectors), pressure or velocity constraints are employed to allow fluxes to be quantified using simple linear algebra.

5.1.2.3 Buckley-Leverett Solution

Equation 1 may be solved via substitution and integration for the position of the CO₂ front as a function of saturation:

$$x_f = \frac{qt}{\phi A} \frac{df}{dS} \quad (5)$$

df/dS can be quantified either analytically or numerically, depending on the form of the relative permeability relationship. However, a discontinuity in this derivative exists at the sharp interface between the two fluids, leading to two sets of saturation values existing as possible solutions both behind and in front of the interface. The common resolution of this issue in solving the Buckley-Leverett equation requires that the position of the sharp front be determined implicitly so that the area under the saturation-versus-distance curve ahead of the front equals area under the same curve behind the front.

The implementation of the multiphase semi-analytical model entails mapping of the one-dimensional Buckley-Leverett solution onto the analytic element-computed fluid flow field. This is accomplished by particle tracking, with an encircling set of particles placed in close proximity to the injector as an initial condition. The subsequent progress of the particles under the influence of the imposed fluid fluxes is tracked using an adaptive linear multistep algorithm to solve the resulting set of coupled ordinary differential equations for particle position. By employing uniform, fixed-sized time steps of Δt , the fluid saturations given by the Buckley-Leverett equation at a given position in a one-dimensional column (implied the product of the uniform fluid velocity and $\Delta t i$, where i is the time-step index number) can be assigned to the corresponding particle location at $\Delta t i$.

Unlike fluid saturation, particle tracking cannot be used to directly map the pressures implied by the one-dimensional Buckley-Leverett solution onto the flow field. Variable fluid composition implies an

effective total fluid permeability (i.e., the sum of the relative permeabilities of each fluid phase at a given saturation state) which changes dynamically as a function of both location and time. Therefore, a simplified heuristic rule set is applied to obtain a partial, approximate pressure correction for multiphase flow with respect to the pure single-phase flow equivalent:

1. The maximum injection pressure for the non-aqueous phase proximal to the injection well, $p_{na,max}$, is given by $p_{w,max} k_{r,na}^* \mu_w k_{r,w}^{-1} \mu_{na}^{-1}$, where $p_{w,max}$ is the calculated injection pressure for with single-phase (water) at the injection well, and $k_{r,na}^*$ the geometric mean relative permeability with respect to the non-aqueous fluid phase across the range of saturation values permitted by the Buckley-Leverett equation solution.
2. The fluid pressure, p_{na} , behind the fluid displacement front is given by $p_{w,i} (p_{na} - p_{w,i}) / R_{i,max} \sum R_i$, where $R_i = \mu_w / k_{r,w}(S) + \mu_{na} / k_{r,na}(S)$, an integrated hydraulic resistance term, summed from the fluid displacement front to the particle location i . $R_{i,max}$ is the sum of the all the resistance terms along the flow path between the fluid displacement front and the injector.
3. Beyond the fluid displacement front, the fluid pressure is simply the single-phase (water) fluid pressure calculated using the analytical element model.

5.1.2.4 Verification

Nordbotten et al. (2005) developed an analytical solution for the injection of supercritical CO₂ into a brine-filled reservoir of uniform thickness and infinite areal extent. The position of the CO₂-water interface is expressed as function of radial distance, depth, and time, assuming a sharp interface between the two fluid phases, with the CO₂ phase placed above the water phase at all radii. This cylindrical model collapses to a radial model via normalizing the vertical thicknesses of the CO₂ and brine phases at a given radial distance, yielding an effective CO₂ saturation as a function of radial distance and time. A comparison the semi-analytical model and the Nordbotten et al. (2005) solution (Figure 6.4.1) indicates excellent agreement.

5.1.2.5 Application

The Paleozoic Knox formation, a carbonate reservoir found in the Illinois Basin in the Midwestern U.S., is a proposed target for CO₂ storage (Figure 6.4.2). To address the issue of potential injection-induced seismicity along nearby inferred strike slip faults, a set of Monte Carlo simulations were conducted using the semi-analytical model to constrain possible values of fluid pressure increases along the faults, given (limited) geologic data and an assumed CO₂ injection flux of 1 MT/yr. Model results were compared to those generated by a three-dimensional, multiphase finite difference simulation which posited heterogeneous distributions of permeability and porosity applicable to carbonate rocks (Figures 6.4.3 and 6.4.4). The CO₂ saturation and fluid pressure for a baseline case representing mean parameter values from the finite difference model are shown for comparison on Figure 6.4.5. The 70th percentile value for the permeability field in each of the finite difference models was used to represent the mean permeability to account for the effects of preferential flow pathways connecting the model interior to the fixed pressure boundaries.

For the Monte Carlo realizations, 1,000 individual simulations were generated with the semi-analytical model, with k_x selected from a lognormal distribution (log mean = 10 mD; $\sigma = 1$), k_y a fraction of k_x ranging between 0.2 and 0.1, the orientation of the principal permeability with respect to the x-axis ranging between 0 and 75 degrees, b ranging between 100 and 600 m, k_c chosen from a simple log uniform distribution (10^{-5} to 10^{-1} mD), and b_c ranging between 500 and 1,000 m. A random subset of the resulting implied fluid pressures along the most proximal fault to the injector as well as in the vicinity of the injection well versus permeability are shown on Figure 6.4.6. Cumulative probability distributions for the full set of modeled fluid pressures (Figure 6.4.7) provide an indication of the nature of the uncertainty associated with these model predictions. When combined with regional stress tensor data, these results will allow for more quantitative insights into the overall probability of induced seismicity events.

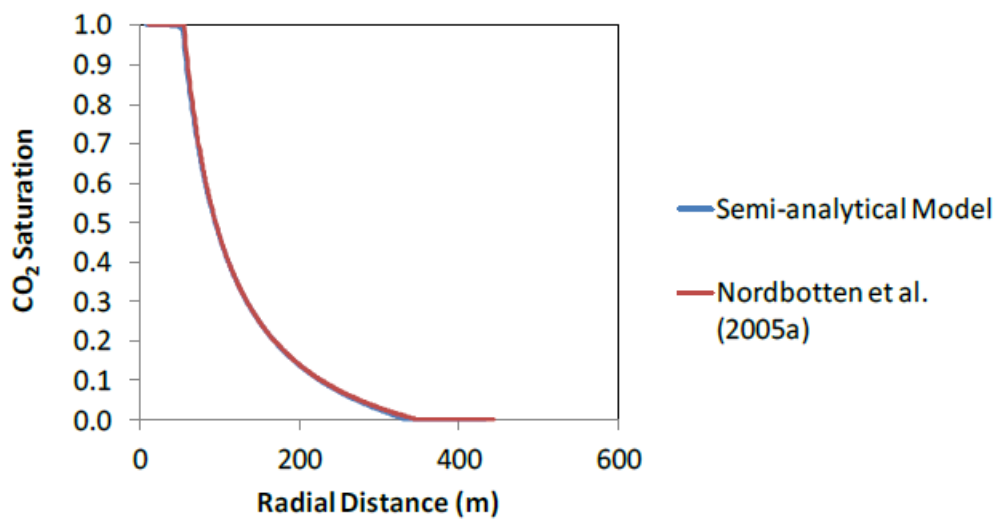


Figure 6.4.1. Modeled radial CO₂ saturation ($t = 4$ years; $k_r = S$ for both fluids; $k = 10$ mD; $Q = 0.04$ MT/yr CO₂; $b = 20$ m; $\phi = 0.2$; $\mu_w = 2.5 \times 10^{-4}$ Pa·sec; $\mu_{CO_2} = 3.95 \times 10^{-5}$ Pa·sec) as predicted by the semi-analytical solution of this study versus the analytical solution proposed by Nordbotten et al. (2005). The two profiles fully overlap.

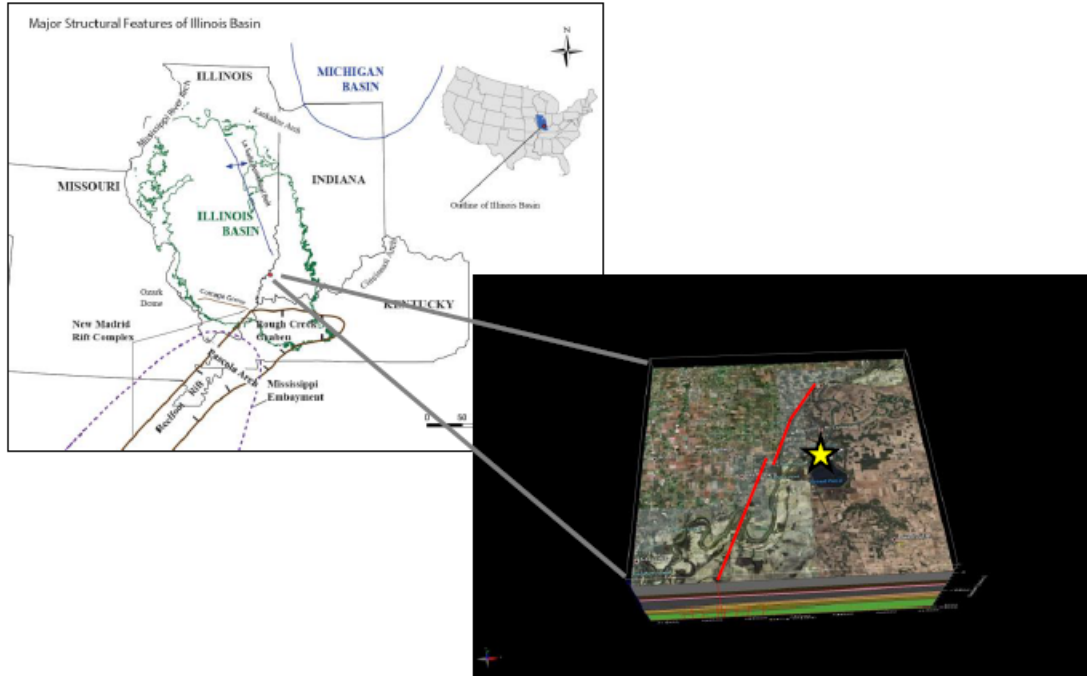


Figure. 6.4.2. Gibson-3 site location in the Illinois Basin, southwest Indiana, with regional fault segments indicated in red and injection site by yellow star symbol.

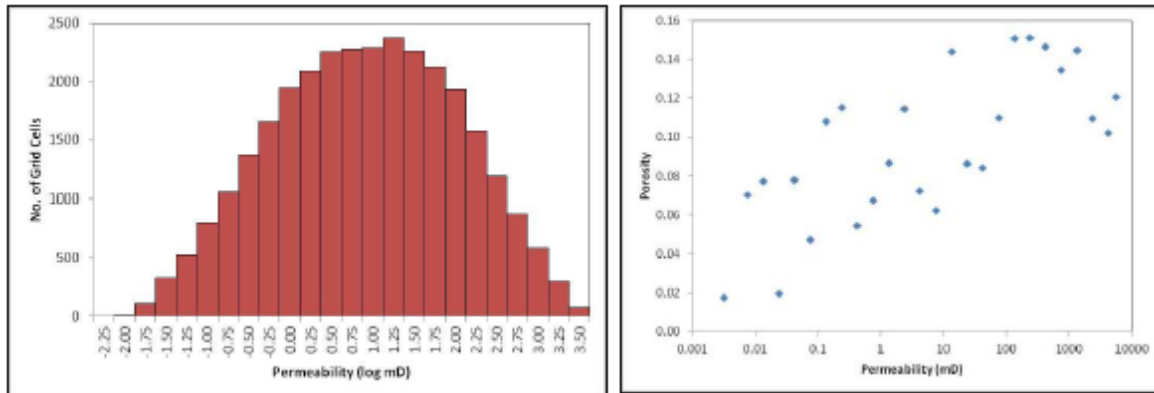


Figure 6.4.3: Probability distribution of permeability (left) and posited porosity-versus-permeability correlation (right) for targeted carbonate reservoir.

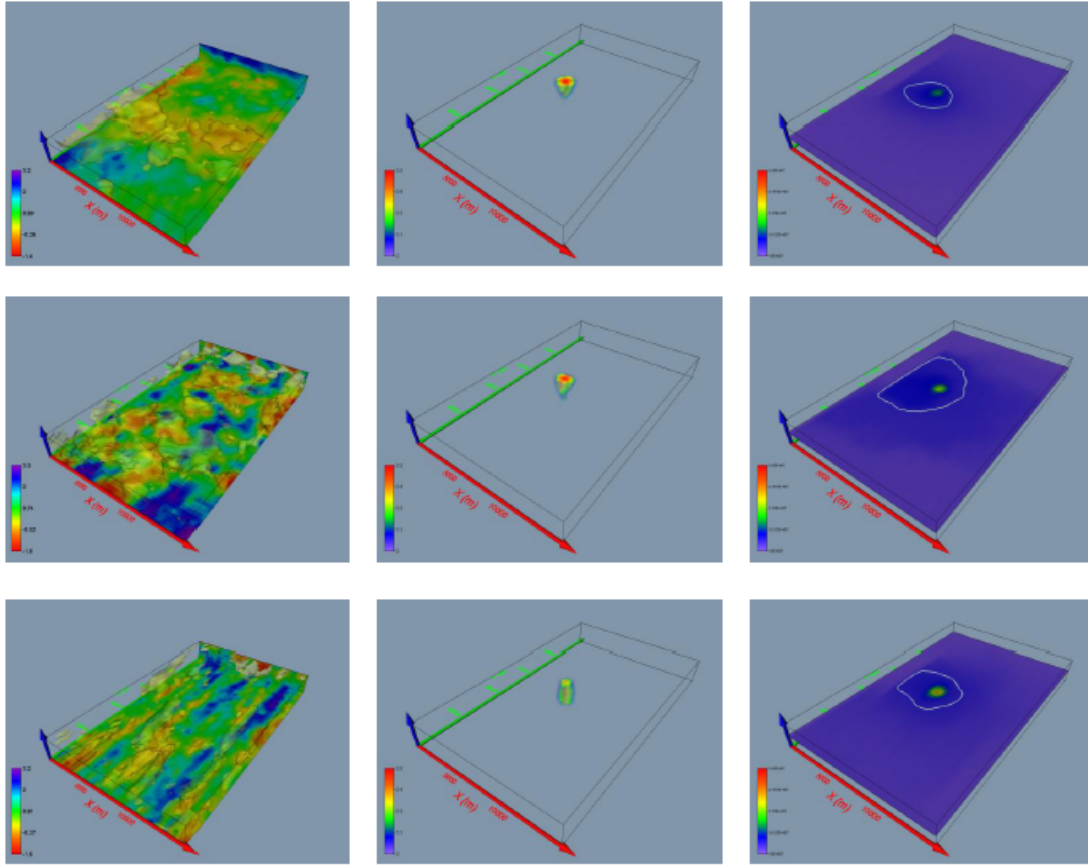


Figure 6.4.4: Permeability field realizations (left column), modeled CO₂ saturations after 10 years of injection (middle column), and the corresponding fluid pressures at the middle depth of the reservoir (right column; white contour line corresponds to 18 MPa), 15 km x 25 km x 300 m system. Constant pressure (hydrostatic) boundary conditions exist approximately 30 km in each direction beyond the interior model domain depicted in the plots. Interior domain discretization consists of 60 x 100 x 5 cells in the x-, y-, and z-directions. Vertical exaggeration = 10X.

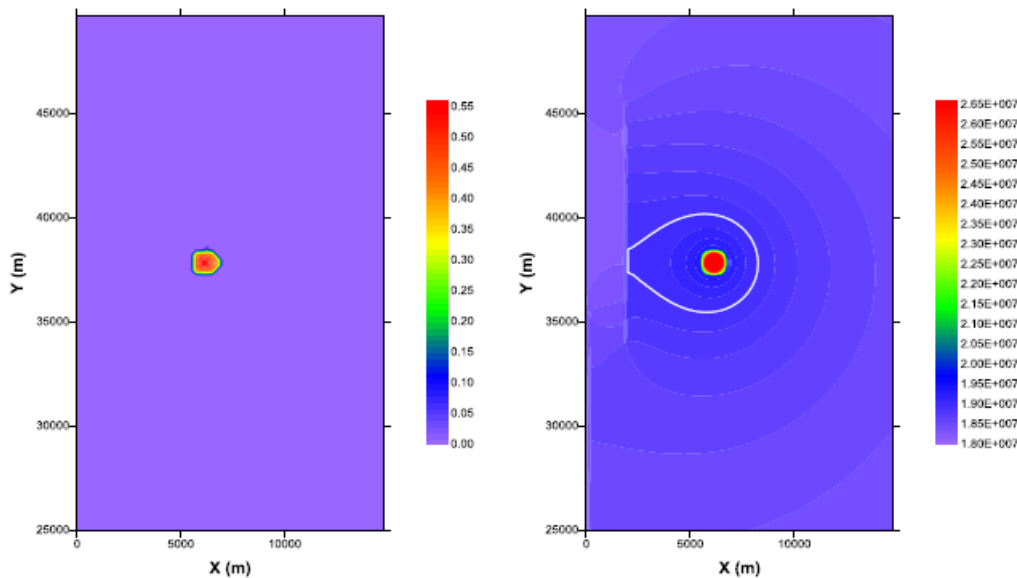


Figure 6.4.5: CO2 saturation (left) and fluid pressure (right) after 10 years of injection, simulated using the semi-analytical model; $k_x = k_y = 25$ mD, $\phi = 0.1$, $b = 300$ m, $bc = 500$ m, and $k_c = 10$ μ D. White contour line corresponds to 18 MPa; pressure color scale ranging from 18 MPa to 26.5 MPa corresponds to the pressure ranges indicated on the right column of Figure 3.

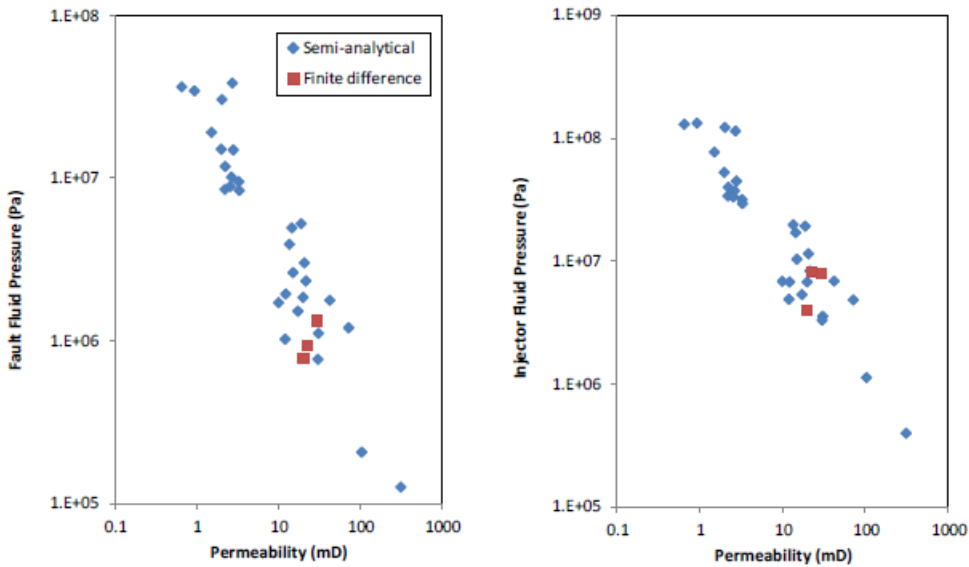


Figure 6.4.6: Subsets of modeled maximum fluid pressures along the northernmost fault (left) and the near the injection well (right) versus characteristic permeability, represented by the geometric mean of k_x and k_y (semi-analytical model) or the 70th percentile permeability in the heterogeneous fields (finite difference models).

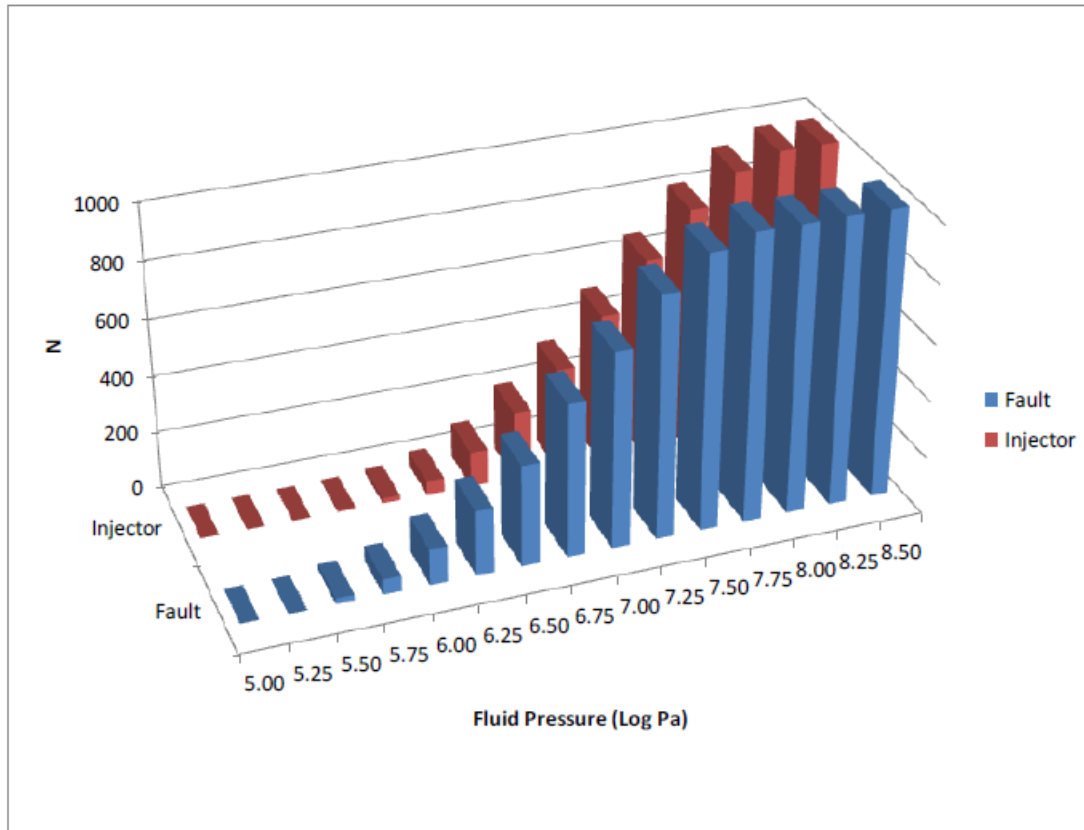


Figure 6.4.7: Probability distributions of modeled maximum fluid pressure at the northernmost fault extension and fluid pressure in the vicinity of the injection well.

5.1.2.6 Plans for Upcoming Quarter

A second approach for enhancing the computational efficiency of CO₂ injection and storage simulations, but one which encompasses a broader set of physical as well as geochemical processes is to employ a multiphase flow and transport model emulator. Emulation is based on the generation of a response surface using a process model (e.g., LLNL’s NUFT code) which is trained from a suite of simulations. The PSUADE code is currently being tested as an emulator for NUFT, with the computational procedure consisting of the following steps:

1. Determine the key n input parameters and their associated uncertainty range (e.g., caprock permeability ranging between from 10^{-16} and 10^{-19} m²) and distribution (e.g., uniform, log-normal).
2. Sample the n parameters in hyper-dimension space (n -dimension), constrained by the range. PSUADE features a suite of sampling methods, including the frequently used Latin hypercube.
3. Employ these sampled parameters in the physical model (e.g. NUFT) as part of a large suite of simulations.
4. Design an objective function and quantify it from the simulation output (e.g., example: maximum overpressure on a fault plane, or surface CO₂ leakage). The input samples and the objective function

represent the training data for PSUADE to construct response surfaces. There are approximately ten types of response surfaces in PSUADE. Typically, the MARS (Multivariate Adaptive Regress Spline) is chosen as a non-parametric surface while a higher order Polynomial Regression Model is chosen as parametric response surface (i.e, can be expressed through mathematic equations).

During the next quarter and throughout FY13, we will develop and apply the emulator approach to address key CO₂ injection and storage issues for the Gibson-3 site and the other two candidate injection locations, leveraging the high degree of both computational efficiency (from a trained model) and process fidelity:

- Sensitivity analysis: identify and quantify parameter contributions to the uncertainty of objective function.
- Prediction: operational parameters (e.g., injection rate, time) can be included in the analysis and used to construct polynomial regression emulators. Given the injection rate and time, the objective function (e.g., fault overpressure) can be predicted with an associated confidence interval with minimal computational effort.
- Optimization: if hydrological parameters and geometric parameters (e.g., well lengths) are included in the analysis, the emulator can be used in CO₂ injection and storage site selection and design.
- Bayesian calibration with observations: by employing a Markov Chain Monte Carlo algorithm, the probability distribution functions of posterior parameter distributions can be calculated, given the large number of model runs which can be conducted using the emulator.

Methodology and results will be shared with our Chinese partners in the CERC technical review in January 2013.

5.1.3 FY13 Q1 (October 1 – December 31, 2012)

During the past quarter, LLNL’s modeling efforts under Subtask 6.4a have continued focused on understanding the constraints on injection at the proposed Gibson-3 storage site in the Illinois Basin. We have built upon previous multiphase flow and transport modeling efforts to construct a reactive transport model for injection into the predominantly carbonate Paleozoic Knox Formation to assess the potential roles of chemical reactions in altering injectivity through changes in porosity and permeability:

$$\frac{dn}{dt} = -S \cdot k_{298.15} \cdot e^{-E/R(T-298.15)} \left(1 - \frac{Q}{K} \right) \quad (\text{Eq. 6.4.1})$$

where (dn/dt) is the change in mineral mass per unit time, S the mineral specific surface area, $k_{298.15}$ the published dissolution rate estimate under ambient conditions, T the temperature, Q the solution saturation index with respect to a given mineral phase, and K the equilibrium constant. The impact to permeability, k , with respect to its initial value, k_0 , is given, in turn, by $k/k_0 = (\phi/\phi_0)^b$, where ϕ is porosity, calculated via Equation 6.4.1 and the respective mineral molar volume, with an appropriate value of the exponent b chosen for a carbonate reservoir.

Example simulation results for a single set of posited hydrologic and geochemical reaction parameter values are shown on Figures 6.4.1 through 6.4.5, assuming the brine chemistry and mineralogy indicated on Table 6.4.1. For this parameter set, changes in permeability and porosity near the injection well are apparent after an injection period lasting some 50 years. However, results are sensitive to assumptions concerning both hydrology and geochemistry. Moreover, individual simulation run times are computationally burdensome, rendering a conventional Monte Carlo-based approach to assign probabilistic forecasts to model results and to assess parameter sensitivity impractical. In response, we are applying the PSUADE emulator to serve as a proxy for the discretized multiphase reactive transport model, which will generate reservoir behavioral predictions based on an objective function response surface. Current research entails “training” the PSUADE model (e.g., generating the response surface) using multiple runs of LLNL’s multiphase, multicomponent reactive transport simulator, NUFT.

5.1.3.1.1 Plans for the Next Quarter

Probabilistic forecasts and parameter sensitivity for reservoir responses to CO₂ injection – both pressure field and geochemistry – generated by PSUADE results and semi-analytical modeling (discussed in prior quarterly updates) will be summarized for the Gibson-3 site. We will then extend these modeling approaches to include a third fluid phase – oil – to address similar reservoir performance questions once enhanced oil recovery is included in the simulations as an injection option. Following application to other site(s) in the Illinois Basin, we will apply these same methodologies to locations in the Ordos Basin, China, in concert with our Chinese CERC collaborators.

Table 6.4.1. Reactive transport model components.

Species	Molality
pH	5.8
Ca ²⁺	0.3
Mg ²⁺	0.12
SO ₄ ²⁻	0.015
Cl ⁻	1.0
Calcite fraction in solid	0.2
Dolomite fraction in solid	0.5

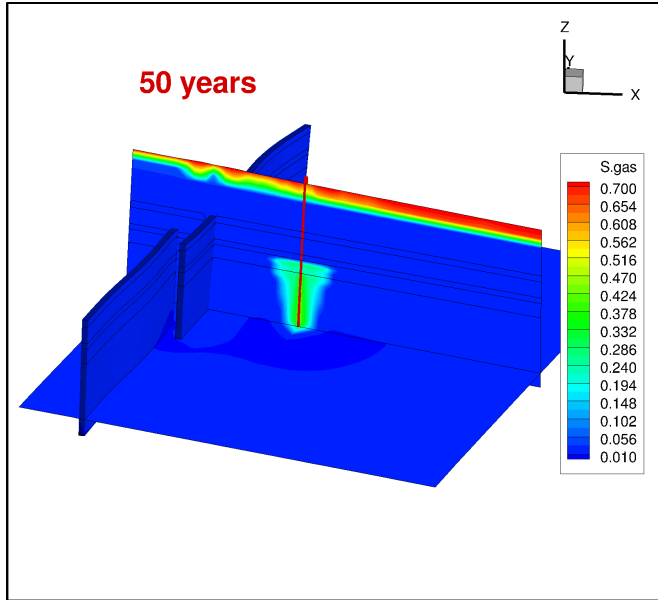


Figure 6.4.1. Simulated CO₂ saturation distribution after 50 years of injection at 1 MT/yr into in the Knox Formation beneath the Gibson-3, reflecting a single parameter set realization.

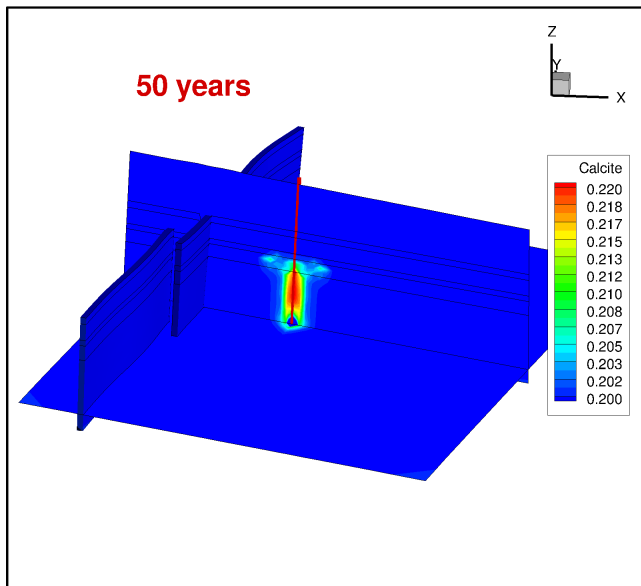


Figure 6.4.2. Simulated distribution of the calcite mineral fraction after 50 years of injection at 1 MT/yr into in the Knox Formation beneath the Gibson-3, reflecting a single parameter set realization.

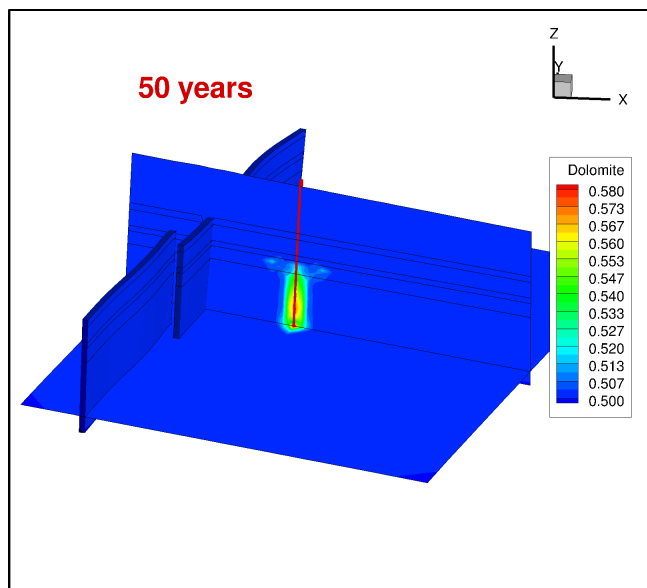


Figure 6.4.3. Simulated distribution of the dolomite mineral fraction after 50 years of injection at 1 MT/yr into in the Knox Formation beneath the Gibson-3, reflecting a single parameter set realization.

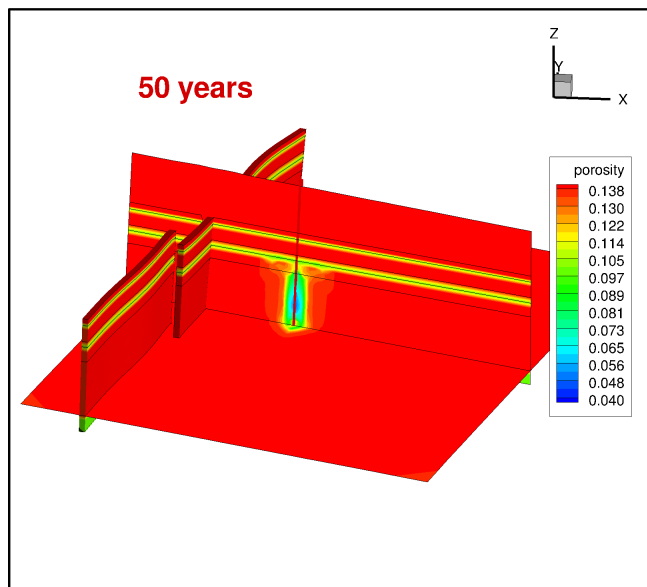


Figure 6.4.4. Simulated distribution of porosity as impacted by carbonate mineral precipitation/dissolution reactions after 50 years of injection at 1 MT/yr into in the Knox Formation beneath the Gibson-3, reflecting a single parameter set realization.

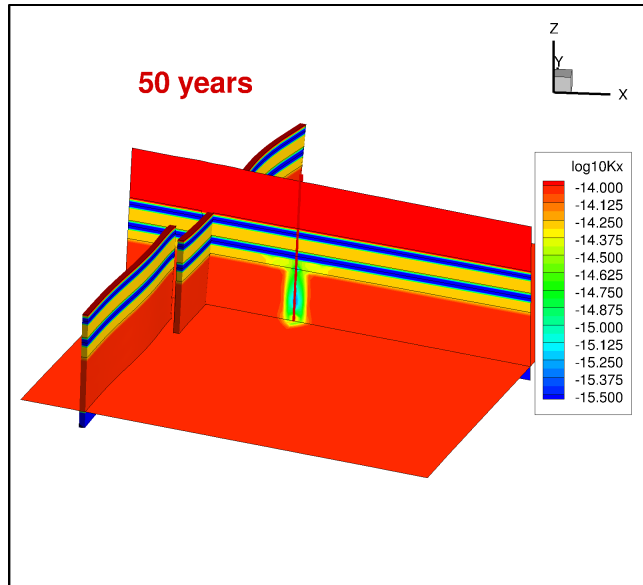


Figure 6.4.5. Simulated distribution of permeability as impacted by carbonate mineral precipitation/dissolution reactions after 50 years of injection at 1 MT/yr into in the Knox Formation beneath the Gibson-3, reflecting a single parameter set realization.

5.1.4 FY13 Q2 (January 1 – March 31, 2013)

No activity on Subtask 6.4a this quarter.

5.1.4.1 Relevant higher-level activity in CERC-ACTC

During the current reporting quarter, the CERC-ACTC held a US-China bilateral workshop in Oakland, California, on January 6-8, 2013. The US internal team held a technical review scheduled consecutive to this meeting, on January 9, 2013. A CERC-wide DOE Steering Committee Meeting was also held in Washington DC on January 10-11, 2013. Pursuant to guidance offered by Secretary Chu at the December 11 meeting, an internal meeting of project partners was held to evaluate the current project portfolio and determine if possible technical redirection was needed. This meeting was held in Washington DC on February 15, 2013.

5.1.5 FY13 Q3 (April 1 – June 30, 2013)

5.1.5.1 Relevant higher-level activity in CERC-ACTC

During the current reporting quarter, the CERC-ACTC US internal team held a final technical review and rescope meeting in Denver, CO, on April 30, 2013. The primary outcome of this meeting was a general reduction in scope on the geologic storage portion of our work, driven by feedback from our industrial partners and the DOE. Work was refocused into improving capture technologies, efficiency improvements, and program development. This activity is still ongoing, and any changes are incorporated into the Year 4 DOE continuation request, which was submitted June 30, 2013

5.1.5.2 Results and Discussion

Recent work by Liu et al. (2013) explored the potential for the New Albany Shale formation in the Illinois Basin to serve as a geologic storage unit for CO₂ while also providing natural gas production via enhanced gas recovery (EGR). IGS work this quarter focused on beginning to incorporate this novel storage option into the broader techno-economic assessment for Gibson-3 by developing new maps of target member thicknesses within the larger New Albany Shale formation. IGS also developed initial maps of total organic carbon content which serves as a proxy for estimating CO₂ storage and CH₄ recovery via the adsorption process.


5.1.5.3 Plans for Upcoming Quarter

IGS plans to evaluate the Schmoker methodology for estimating TOC against core analyses where available and provide the simulation modeling teams with updated spatial data sets of storage potential and methane recovery potential for incorporation into their analysis.

5.2 Presentations

5.2.1 November 2012 Conference Poster

This poster was presented at the International Conference on Greenhouse Gas Technologies, Kyoto, Japan, November 18, 2012 through November 22, 2012. The format has been modified to fit in this document.



Simulating CO₂ Injection and Storage with Limited Site Data: the Utility of a Variably Complex Modeling Approach

Walt McNab^{1,}, Mingjie Chen¹, John Rupp², Kevin Ellett², and Jeff Wagoner¹*

¹Lawrence Livermore National Laboratory, P.O. Box 808, Livermore, California, 94551, U.S.A. (mcnab1@llnl.gov)
²Indiana Geological Survey, 611 N. Walnut Grove, Bloomington, Indiana, 47405, U.S.A

LLNL-POST-600472

Abstract

A semi-analytical model for simulating injection of an immiscible fluid into a water-filled reservoir is developed which approximates the effects of vertical or horizontal injection wells, impermeable fault segments, and permeability anisotropy on phase saturation and fluid pressure. The modeling approach is based upon (1) an analytic element model for single-phase flow associated with specified flux, specified pressure, and impermeable line-segment elements within a reservoir of uniform thickness and porosity, (2) an analytical solution to the one-dimensional Buckley-Leverett equation for immiscible displacement of one fluid by another in porous media, subject to relative permeability functions dependent on fluid saturation, and (3) mapping of the Buckley-Leverett solution onto the two-dimensional flow field using particle tracking. Correction of the computed single-phase pressure distribution behind the fluid displacement front for two-phase flow is accomplished using a heuristic model. Application of the model to a proposed geological CO₂ storage system in the Illinois Basin, U.S.A., characterized by an injection zone that is proximally cut by extensions of a regional fault system, includes assessments of the impact of permeability, anisotropy, and other reservoir characteristics on fluid pressure distributions along the fault segments.

Semi-analytical Model

A computationally-efficient screening tool for CO₂ storage problems is based upon mapping the Buckley-Leverett solution for 1-D immiscible fluid displacement, via particle tracking, to a fluid flow field determined by an analytic element model. A set of heuristic rules are used to adjust fluid pressures as a result of changing fluid saturations. The analytic element approach allows the effects of simple flow heterogeneities to be addressed through the use of integrated line sources and doublets to represent either vertical or horizontal injectors and impermeable faults. Simplifying assumptions include a two-dimensional reservoir of uniform thickness and anisotropic permeability, a leaky confining layer or cap rock, and steady-state, incompressible, fixed-viscosity fluid injection or withdrawal. Buoyancy and capillary forces are neglected.

Buckley-Leverett Solution

The simplest conceptual model for multiphase flow is immiscible fluid displacement in the absence of capillary pressure, as described by the Buckley-Leverett equation:

$$\frac{\partial S}{\partial t} = \frac{Q}{\phi A} \frac{df}{dS} \frac{\partial S}{\partial x}$$

where S is fluid saturation, ϕ the porosity, A the cross sectional area, and f the fluid flow fraction of a non-aqueous phase displacing water:

$$f = \frac{1}{1 + \frac{k_{r,na} \mu_w}{k_{r,w} \mu_{na}}}$$

The Buckley-Leverett equation can be solved analytically for the limiting one-dimensional case when capillary forces are neglected. Saturation distribution is mapped onto the flow field (below) by particle tracking.

Flow model

A modified analytic element methodology is employed which allows for a leaky confining layer, based on the superposition of pressure-influencing terms includes:

$$\Delta P = \frac{Q\sqrt{p}}{2\pi \frac{k_x}{b} K_0} \left(\sqrt{\Delta x^2 + p\Delta y^2} \sqrt{\frac{k_c}{k b b_c}} \right) \quad \text{(Single point source; DeGlee, 1930)}$$

$$\Delta P = \frac{Q\sqrt{p}}{2\pi \frac{k}{b} \int_{x=x_i}^{x=x_f} \frac{\Delta x dx}{\sqrt{\Delta x^2 + p\Delta y^2}}} \quad \text{(Doublet element)}$$

where Q is the injection rate, k the reservoir permeability tensor, k_c the cap rock permeability, μ the fluid viscosity, b the reservoir thickness, b_c the cap rock thickness, $p = k_r/k_y$, and Δx and Δy are distance offsets. Equations are solved for each element by both analytical and numerical integration.

Heuristic model for pressure correction

1. Maximum injection pressure for the non-aqueous phase proximal to the injection well, $p_{na,max}$, is given by $p_{w,max} \cdot k_{r,na} \cdot \mu_w \cdot k_{r,w}^{-1} \cdot \mu_{na}^{-1}$, where $p_{w,max}$ is the calculated injection pressure for with single-phase (water) at the injection well, and $k_{r,na}$ the geometric mean relative permeability with respect to the non-aqueous fluid phase across the range of saturation values permitted by the Buckley-Leverett equation solution.
2. Fluid pressure, p_{na} , behind the displacement front is given by $p_{w,i} (p_{na} - p_{wi}) / R_{i,max} \cdot \sum R_i$ where $R_i = \mu_w k_{r,w}(S) + \mu_{na} / k_{r,na}(S)$, an integrated hydraulic resistance term, summed from the displacement front to the particle location i . $R_{i,max}$ is the sum of the all the resistance terms along the flow path between the fluid displacement front and the injector.
3. Beyond the fluid displacement front, the fluid pressure is simply the single-phase (water) fluid pressure calculated using the analytical element model.

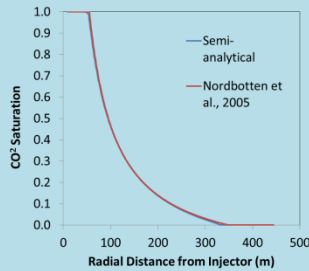


Figure 1: Validation test problem - modelled radial CO₂ saturation (t = 4 years; k_r = S for both fluids; k = 10 mD; Q = 0.04 MT/yr CO₂; b = 20 m; ϕ = 0.2; μ_w = 2.5 x 10⁻⁴ Pa·sec; μ_{CO2} = 3.95 x 10⁻⁵ Pa·sec) as predicted by the semi-analytical solution of this study versus the analytical solution proposed by Nordbotten et al. (2005). The two profiles fully overlap.

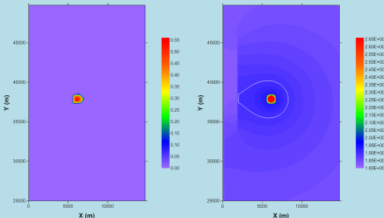


Figure 2: Plan-view CO₂ saturation (left) and fluid pressure (right) after 10 years of injection, simulated using the semi-analytical model; k_x = k_y = 25 mD, ϕ = 0.1, b = 300 m, b_c = 500 m, and k_c = 10 μ D. White contour line corresponds to P = 18 MPa; pressure color scale ranging from 18 MPa to 26.5 MPa corresponds to the pressure ranges indicated on the right column of Figure 9.

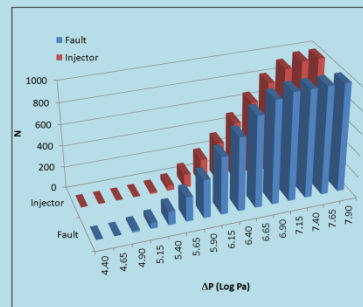


Figure 3: Cumulative probability distributions of modeled maximum fluid overpressure at the northernmost fault extension as well as fluid overpressure in the vicinity of the injection well.

Deterministic Numerical Model

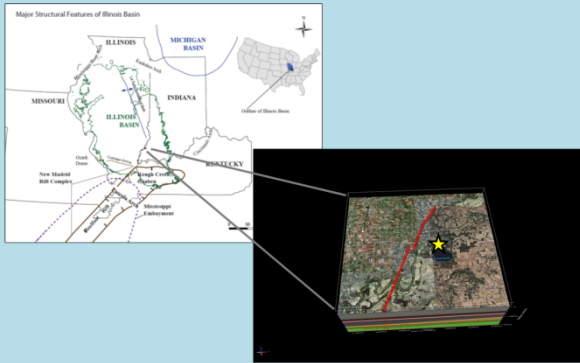


Figure 4: Gibson-3 site location in the Illinois Basin, southwest Indiana, with regional fault segments indicated in red and injection site by yellow star symbol. 3-D model based on local hydrostratigraphy.

System	Series	Group	Formation	Thickness (feet)	Lithology	Graphic Column	Hydrostratigraphic Unit
DEPOSIUM	Upper	New Albany	New Albany	90-200	Black Shale, Brule Shale	[Green]	Aquifer 1
	Middle		20-100	Fine-grained dolomite, sandy dolomite	[Blue]		
	Lower		60-100	Cherty dolomite and dolomite	[Blue]	Aquifer 4	
SILURIAN	Lower	Huntsville or Salina	Huntsville	80-100	Addressed silty dolomite and dolomite with chert	[Blue]	
	Upper		100-150	Cherty dolomite and limestone	[Blue]	Aquifer 3	
ORDOVICIAN	Upper	Maestri	Maestri	200-300	Dolomite and limestone	[Yellow]	Aquifer 2
	Middle		100-150	Dolomite and limestone	[Yellow]		
	Lower		100-150	Dolomite with interbeds of shale, siltstone or sandstone	[Yellow]	Aquifer 2	
CAMBRIAN	Upper	Munich	Munich	80-100	Dolomite, sandstone and dolomite	[Yellow]	Aquifer 1
	Middle		100-150	Subdolomitic shale	[Yellow]		
	Lower		100-150	Subdolomitic sandstone	[Yellow]	Aquifer 1	
PRE-CAMBRIAN			Basement Complex				

Figure 5: Hydrostratigraphic column for the CO₂ injection and storage target reservoir in the Illinois Basin.

Figure 6: An EarthVision geological model was used to construct an integral finite difference mesh (grid plane curved and rotated to conform to faults, variable-sized grid cells) for the multiphase flow simulation.

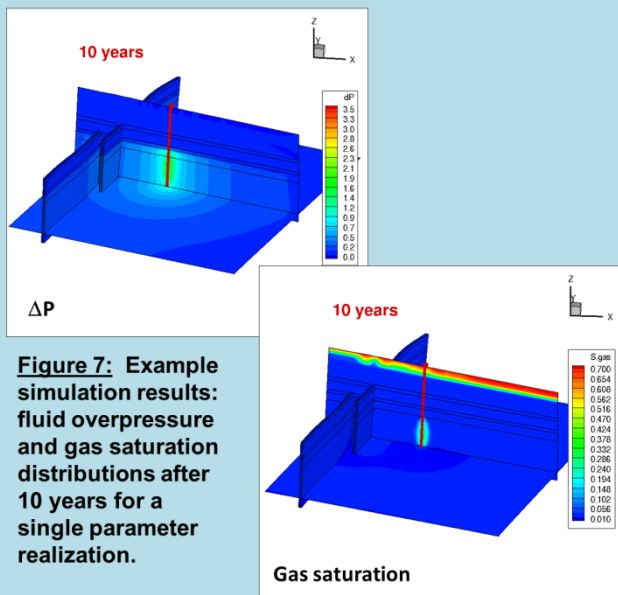
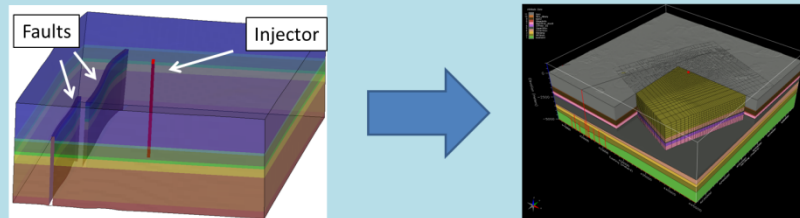


Figure 7: Example simulation results: fluid overpressure and gas saturation distributions after 10 years for a single parameter realization.

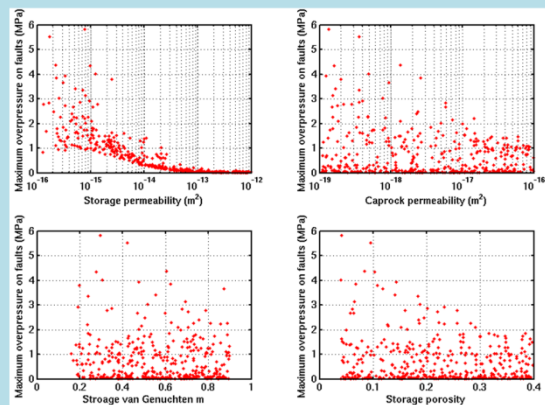
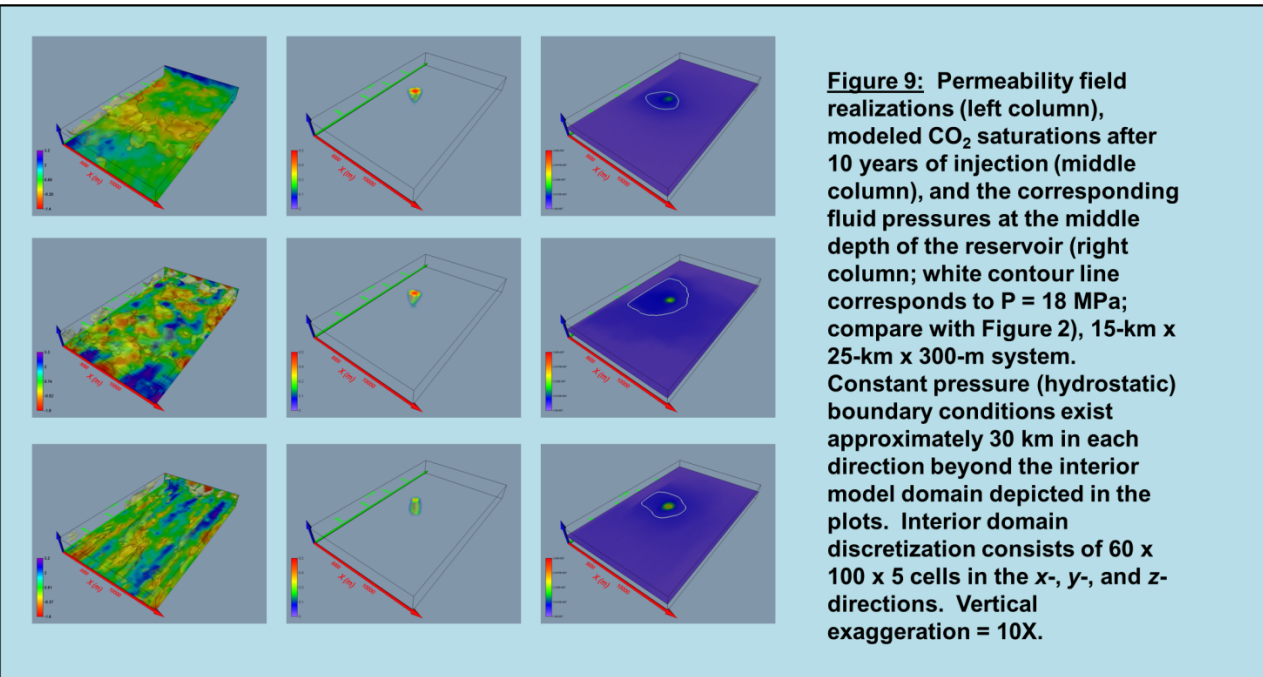


Figure 8: Parameter sensitivity analyses based on discrete model output: fluid overpressure versus reservoir permeability, cap rock permeability, van Genuchten “m” parameter, and reservoir porosity.

Stochastic Numerical Model



Summary of Findings

- Parameter sensitivity for discretized model (500 realizations → days of CPU time in parallel mode) included reservoir, cap rock, adjacent formation permeabilities; relative permeability/capillarity model; porosity; variable pressure boundary conditions.
- Parameter sensitivity for semi-analytical model (1,000 realizations → ~1 hour of CPU time on a single processor) included reservoir and cap rock permeability, anisotropy, effective reservoir thickness.
- Both approaches indicate a mean fault $\Delta P \sim 1$ Mpa, with a greater spread yielded by semi-analytical model.
- Computational efficiency gained using the semi-analytical model validates its proposed role as a useful proxy.

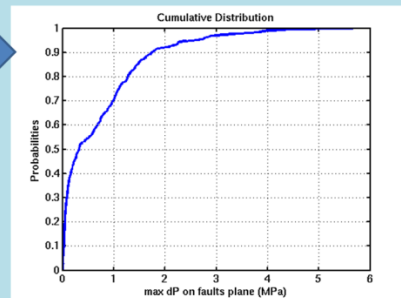


Figure 10: Discrete model maximum fault fluid overpressure probability distribution.

5.2.2 January 2013 Presentation: LLNL Input on Theme 6

This 14-page presentation written January 8, 2013 contains a valuable snapshot of LLNL's progress when funding was curtailed.

THEME 6 – SEQUESTRATION CAPACITY AND NEAR-TERM OPPORTUNITIES

Theme Leads

Dr. Tim Carr – West Virginia University

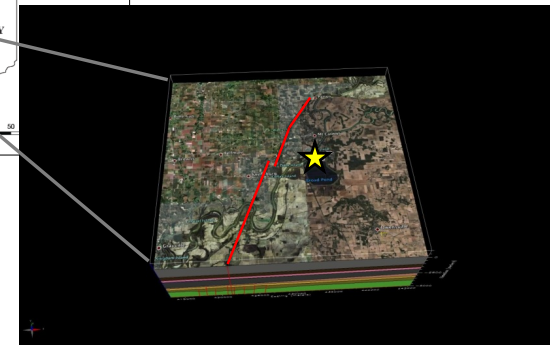
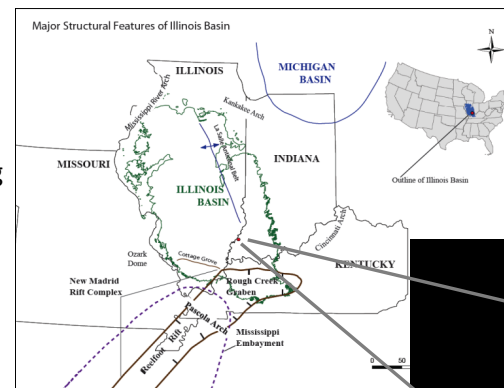
Dr. Ron Surdam – University of Wyoming

Dr. Phil Stauffer - Los Alamos National Laboratory

Dr. Walt McNab - Lawrence Livermore National
Laboratory

Progress and Accomplishments

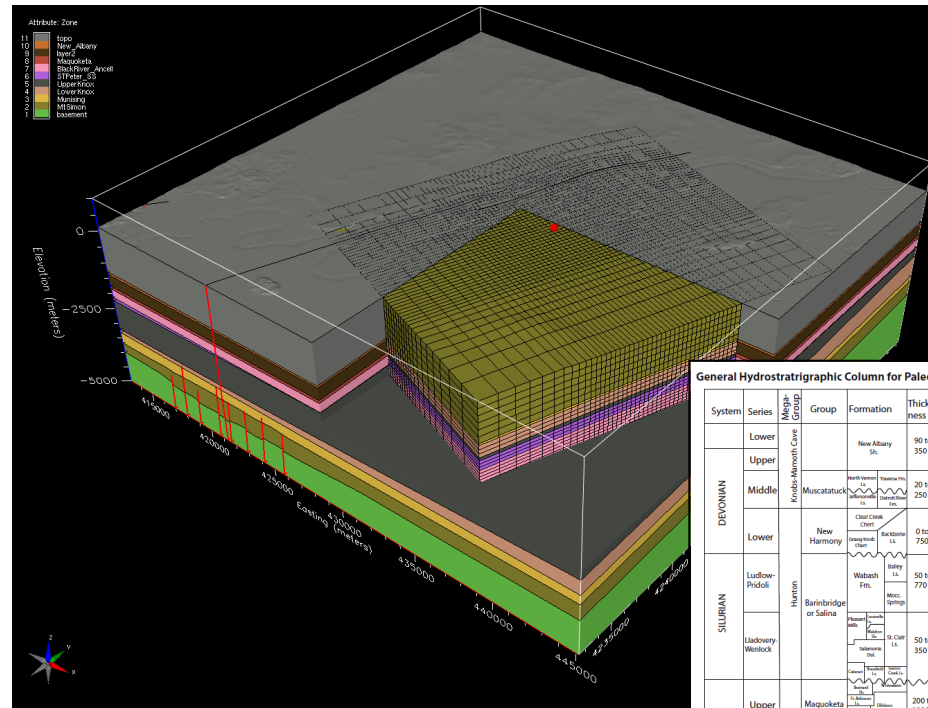
- ▣ New, computationally efficient modeling approaches, applied to Gibson-3 site in Illinois Basin, U.S.A.
 - PSUADE emulator used to streamline probabilistic modeling and parameter sensitivity analyses for multiphase flow and transport and chemical reactions.
 - Semi-analytical model developed for rapid screening of multiphase injection/flow problems.
- ▣ Publications/conferences
 - McNab W, Rupp J, Ellett K, Wagoner J. Simulating CO₂ injection and storage with limited site data: the utility of a variably complex modeling approach, Greenhouse Gas Control Technologies-11 Conference, Kyoto, Japan, November 2012.
 - McNab WW. A semi-analytical model for approximating immiscible fluid injection into a subsurface reservoir with application to CO₂ storage, submitted to *Transport in Porous Media*, 2012 (in revision).



Gibson-3 site location in the Illinois Basin, southwest Indiana, with regional fault segments indicated in red.

Progress and Accomplishments: (1) Multiphase Flow and Transport Modeling

- ▣ Initial NUFT simulation based on site hydrostratigraphy, informed by EarthVision
 - Grid rotated and curved to conform to two major faults.
 - Variable grid block size: 46 x 51 x 30 = 70,380 cells.
 - Injection well located ~4 km east of fault segment.



NUFT model grid.

General Hydrostratigraphic Column for Paleozoic Rocks in Indiana (Cambrian-Mississippian)

System	Series	Member/Group	Formation	Thickness (ft)	Lithology	Graphic Column	Hydrostratigraphic Unit
DEVONIAN	Lower	Knox/Memphian Core	New Albany Sl.	90 to 350	Black Shale, Blocher Shale		Aquifer 4
	Upper						
	Middle	Muscatuck	North Western Indiana Sh. & S. & W. Indiana Sh. & S.	20 to 250	Fine-grained dolomite, Sandy dolomite		
SILURIAN	Lower	Mazon	New Harmony	0 to 750	Cherty limestone and dolomite		Aquifer 4
			Wabash Fm.	50 to 770	Calcareous silty dolomite and dolomitic silty limestone		
		Bainbridge or Salina			Limestone, dolomitic limestone, and dolomite		
	Ludlow-Pidoli				Cherty dolomite and limestone		Aquifer 3
ORDOVICIAN		Onondaga	Ludlow-Wenlock	50 to 350	Cherty dolomite and limestone		Aquifer 3
	Upper		Maquoketa	200 to 1000	Dolomite and limestone, Dolomitic Shale		Aquifer 2
	Middle		Black River	100 to 350	Limestone and shale, Dolomite and dolomitic limestone		
			Ancell	0 to 900	Sandstone and dolomite		Aquifer 2
	Lower	Prairie Du Chien	0 to 2000	Dolomite with interbeds of shale, sandstone			
CAMBRIAN	Upper	Pottsville		20 to 2000	Dolomite with interbeds of shale, siltstone or quartz		
			Munising	50 to 400	Dolomitic sandstones and siltstones		Aquifer 1
PRE-CAMBRIAN	Middle		Eau Claire	400 to 1000	Predominantly shale		
	Lower		Mt. Simon Sl.	250 to 2100	Predominantly sandstone		Aquifer 1
			Basement complex	>1900	Granite, basalt, arkose, and other rocks		

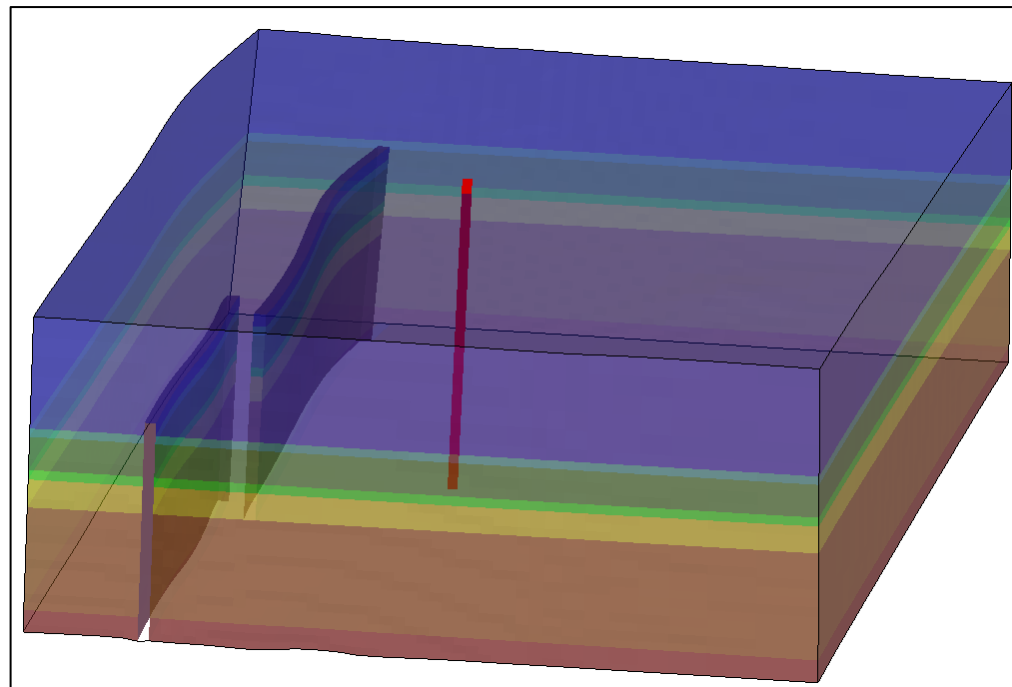
Thicknesses not scaled in proportion to vertical distance

Gibson-3 area stratigraphy.

Progress and Accomplishments: (1) Multiphase Flow and Transport Modeling

▣ Model attributes

- Two phase (gas, liquid), three components (air, water, CO₂), isothermal model.
- Top and bottom boundary conditions based on 1M-year initialization
- CO₂ injected into portions of Knox Formation at 1M tons/yr.

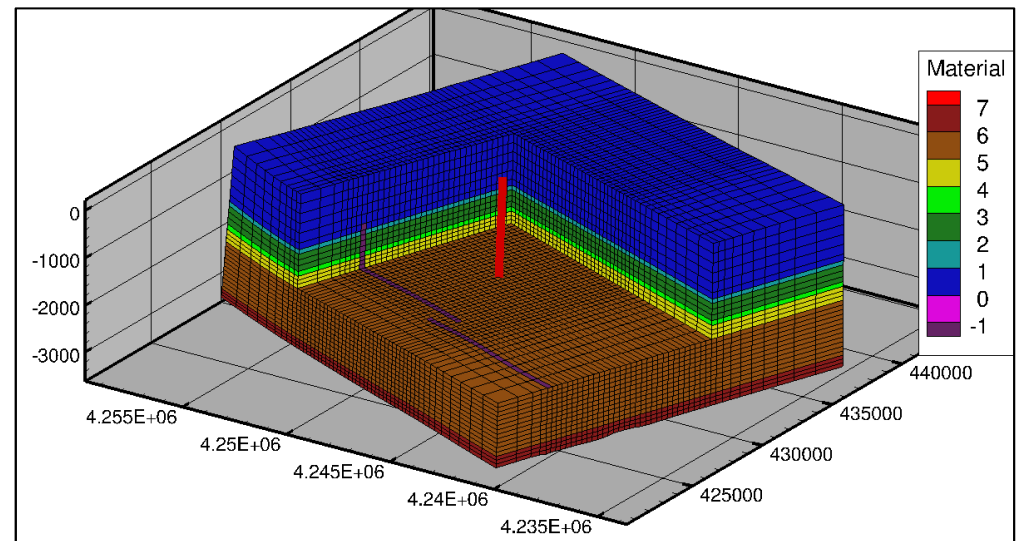


Vertically-exaggerated model domain overview, indicating stratigraphy, faults, and CO₂ injection.

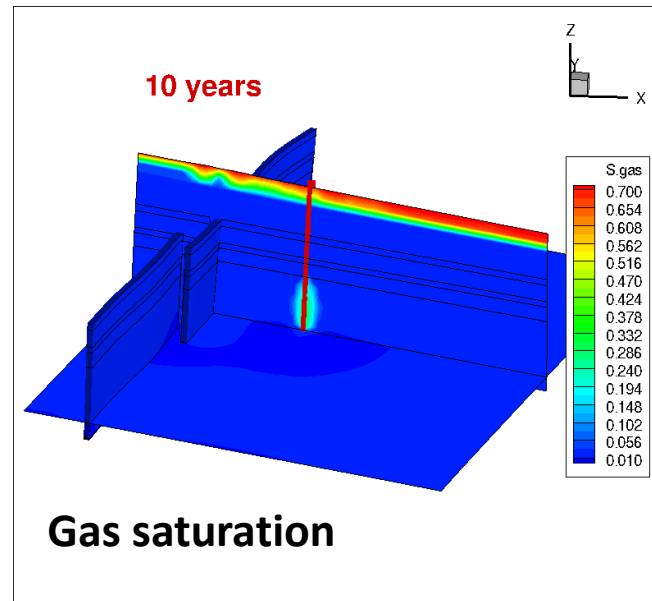
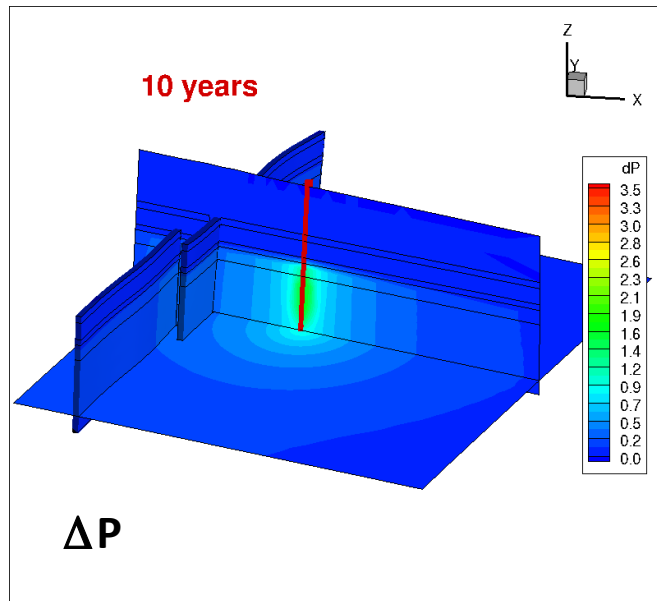
Progress and Accomplishments: (1) Multiphase Flow and Transport Modeling

ID	Name	Property	Thickness (m)	k (mD)	Porosity	Sr_liquid	Sr_gas
1	Topo	Overburden	1250	50.0	0.2	0.2	0.05
2	New Albany	Upper caprock	60	0.01	0.1	0.3	0.166
3	Hunton	Upper aquifer	390	5.0	0.138	0.2	0.1
4	Maquoketa	Lower caprock	100	0.01	0.1	0.3	0.166
5	Blackriver	Storage aquifer	280	5.0	0.138	0.2	0.1
6	Knox	Storage aquifer	1150	10.0	0.138	0.2	0.1
7	Munising	Bedrock	320	0.001	0.1	0.3	0.166

Summary of Flow Model Properties



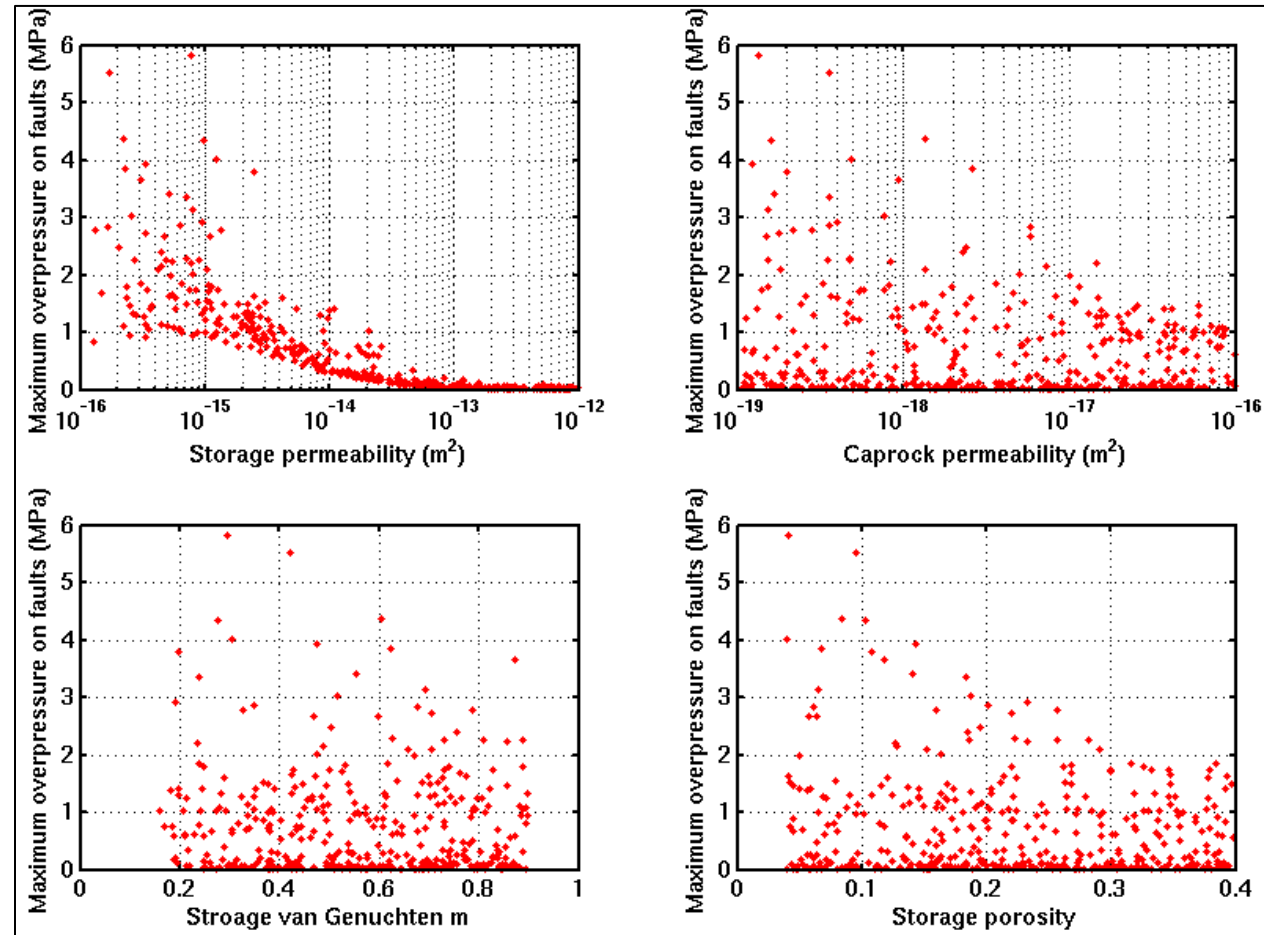
Progress and Accomplishments: (1) Multiphase Flow and Transport Modeling



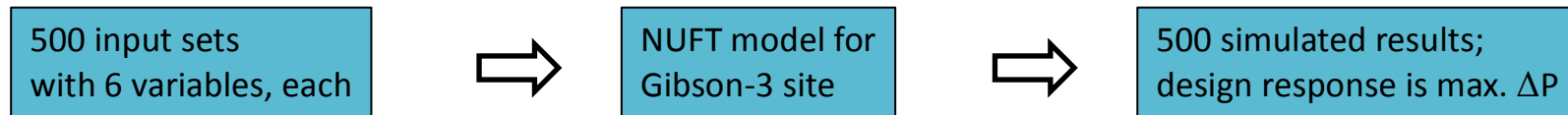
Example simulation results: fluid overpressure and gas saturation distributions after 10 years for a single parameter set realization.

Progress and Accomplishments: (1) Multiphase Flow and Transport Modeling

Parameter sensitivity analyses based on numerical model output: fluid overpressure versus reservoir permeability, cap rock permeability, van Genuchten “*m*” parameter, and reservoir porosity.

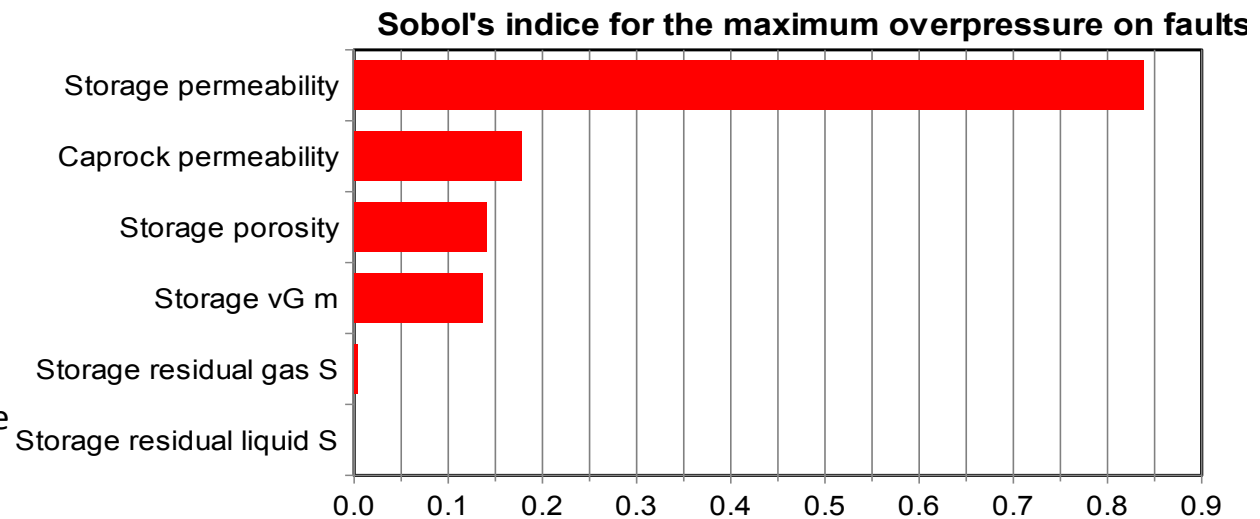


Progress and Accomplishments: (1) Multiphase Flow and Transport Modeling

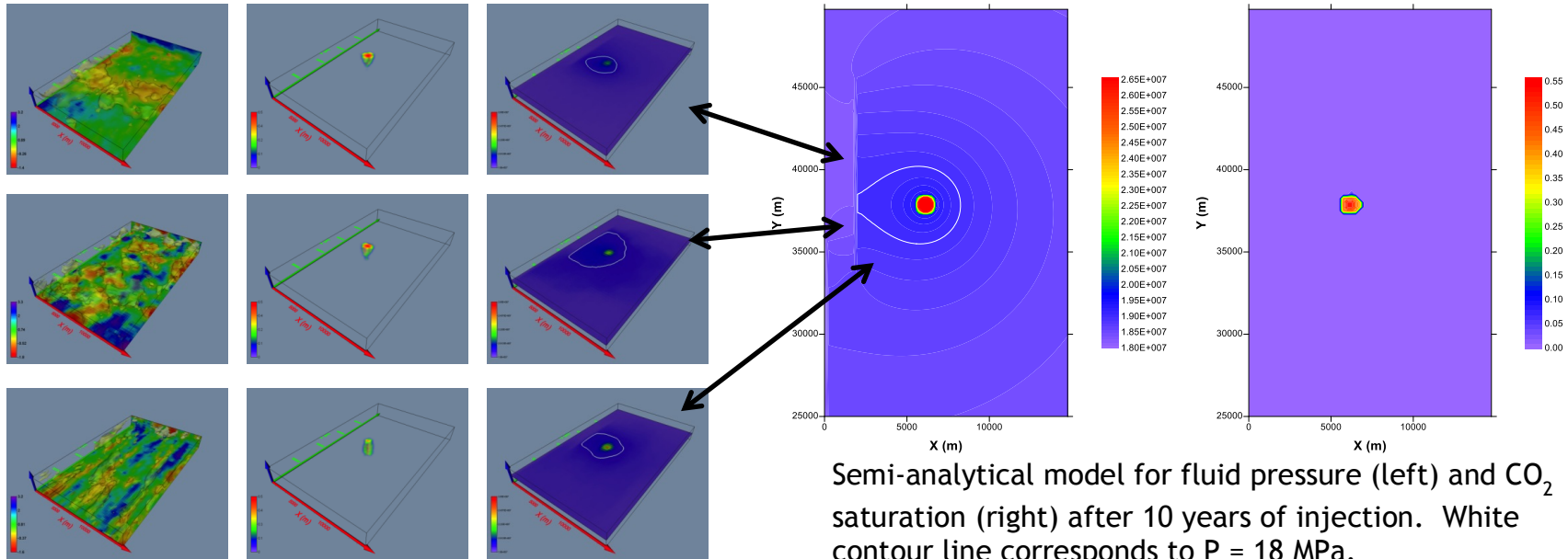


- Emulation (e.g., PSUADE) can replace discretized numerical model (e.g., NUFT)

- Training dataset to build response surface (surrogate model).
- Sensitivity analysis for maximum



Progress and Accomplishments: (2) Semi-analytical Screening Model



Permeability field realizations for a 15-km x 25-km x 300-m model (left column), modeled CO₂ saturations after 10 years of injection (middle column), and the corresponding fluid pressures at the middle depth of the reservoir (right column). White contour line corresponds to P = 18 MPa.

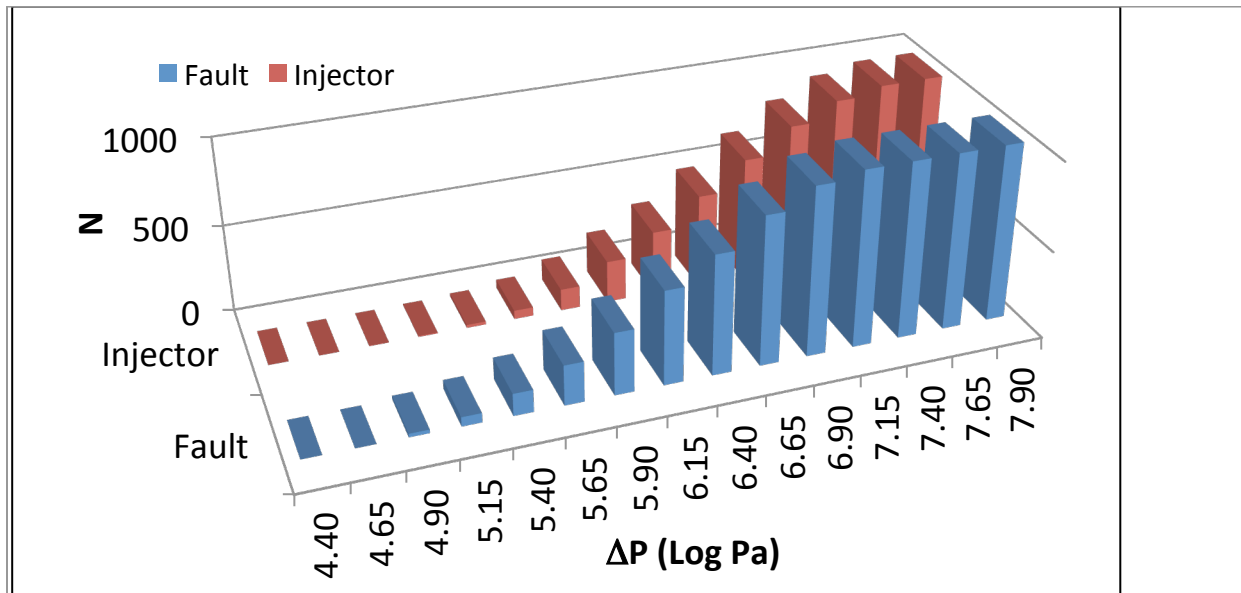
Semi-analytical Approximation for Multiphase Flow Injection

Map solution to the Buckley-Leverett immiscible displacement model onto pressure field calculated using single-phase analytical elements.

$$\frac{\partial S}{\partial t} = \frac{Q}{\phi A} \frac{df}{dS} \frac{\partial S}{\partial x}$$

$$\Delta P = \frac{Q\sqrt{p}}{2\pi \frac{k_x}{\mu} b} K_0 \left(\sqrt{\Delta x^2 + p\Delta y^2} \sqrt{\frac{k_c}{k b b_c}} \right)$$

Progress and Accomplishments: (2) Semi-analytical Screening Model



Semi-analytical model results: Cumulative probability distributions of maximum fluid overpressure at the northernmost fault extension as well as fluid overpressure in the vicinity of the injection well (1,000 realizations). Results compare favorably with multiple-realization numerical model results which require much longer CPU time.

Progress and Accomplishments: (3) Reactive Transport Modeling

Species	Molality
pH	5.8
Ca ²⁺	0.3
Mg ²⁺	0.12
SO ₄ ²⁻	0.015
Cl ⁻	1.0
Calcite fraction in solid	0.2
Dolomite fraction in solid	0.5

Reactions	Log(K _{eq})
CaSO ₄ <=> Ca ²⁺ + SO ₄ ²⁻	-2.236
CO ₂ _aq <=> CO ₂ _g	2.102
HCO ₃ ⁻ + H ⁺ <=> CO ₂ _g + H ₂ O	8.346
MgHCO ₃ ⁺ + H ⁺ <=> Mg ²⁺ + CO ₂ _g + H ₂ O	6.995
MgCl ⁺ <=> Mg ²⁺ + Cl ⁻	0.0695
CaCl ⁺ <=> Ca ²⁺ + Cl ⁻	0.603
CaCl ₂ <=> Ca ²⁺ + 2Cl ⁻	0.667
CaHCO ₃ ⁺ + H ⁺ <=> Ca ²⁺ + CO ₂ _g + H ₂ O	7.002
Calcite + 2H ⁺ <=> Ca ²⁺ + CO ₂ _g + H ₂ O	9.316
Dolomite + 4H ⁺ <=> Ca ²⁺ + Mg ²⁺ + 2CO ₂ _g + 2H ₂ O	18.148

Including reactive chemistry (mineral precipitation/dissolution) in the multiphase flow problem:

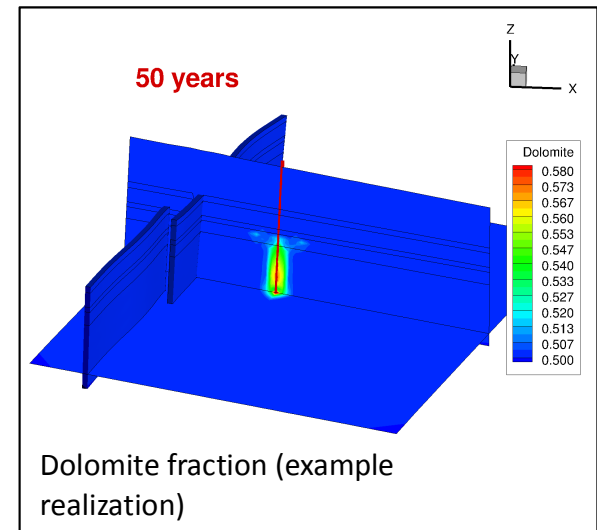
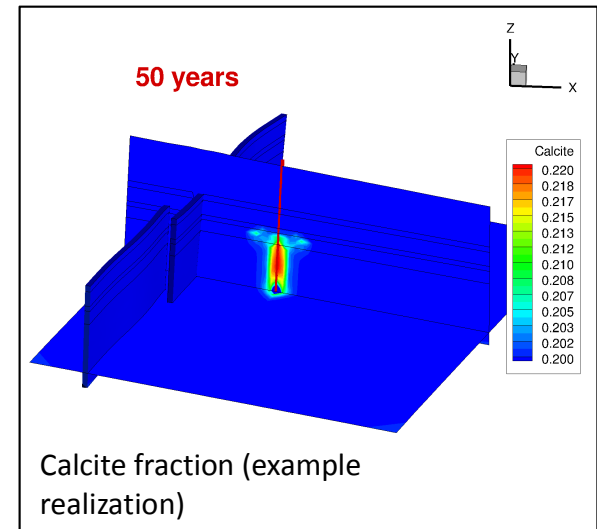
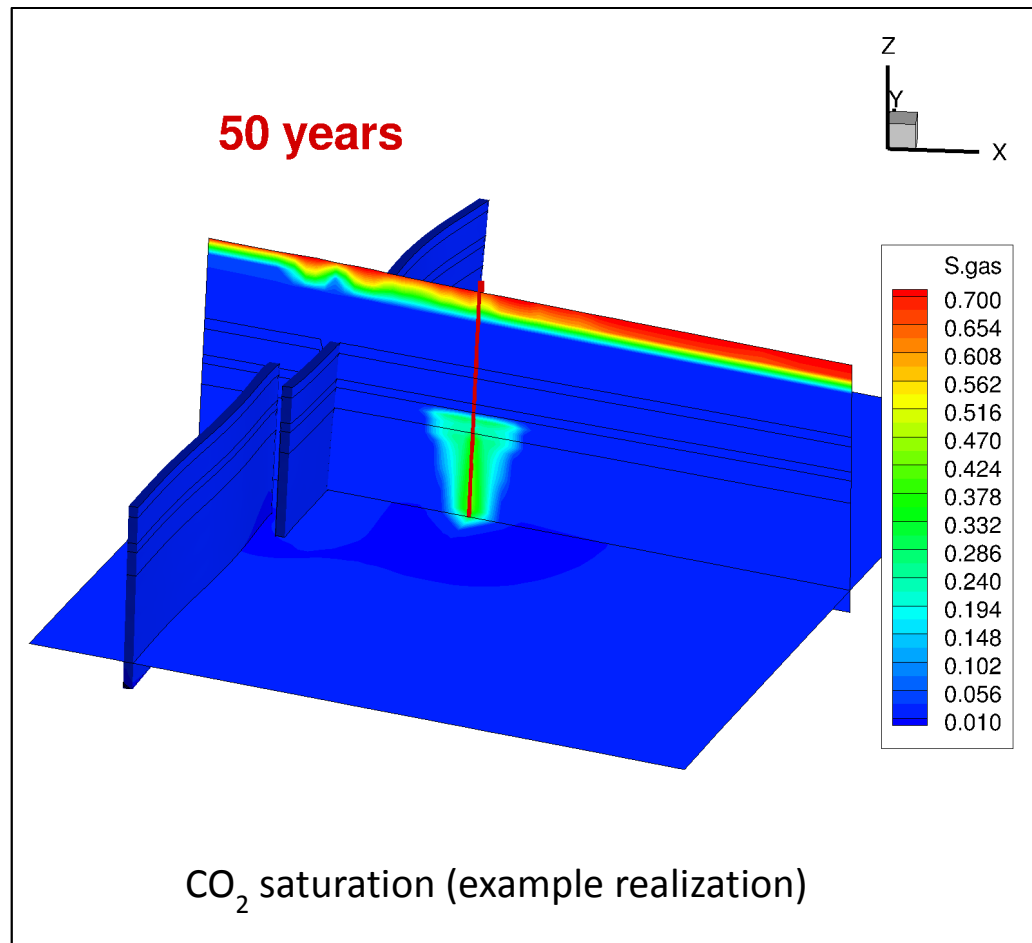
$$\frac{dn}{dt} = -S \cdot k_{298.15} \cdot e^{-E/R(T-298.15)} \left(1 - \frac{Q}{K}\right)$$

and resultant changes in porosity and permeability:

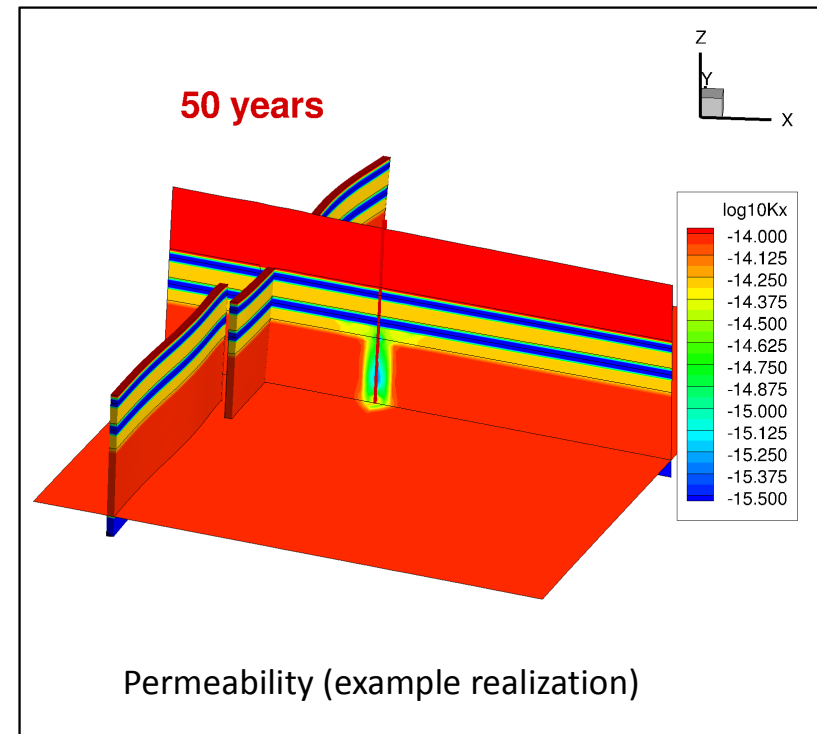
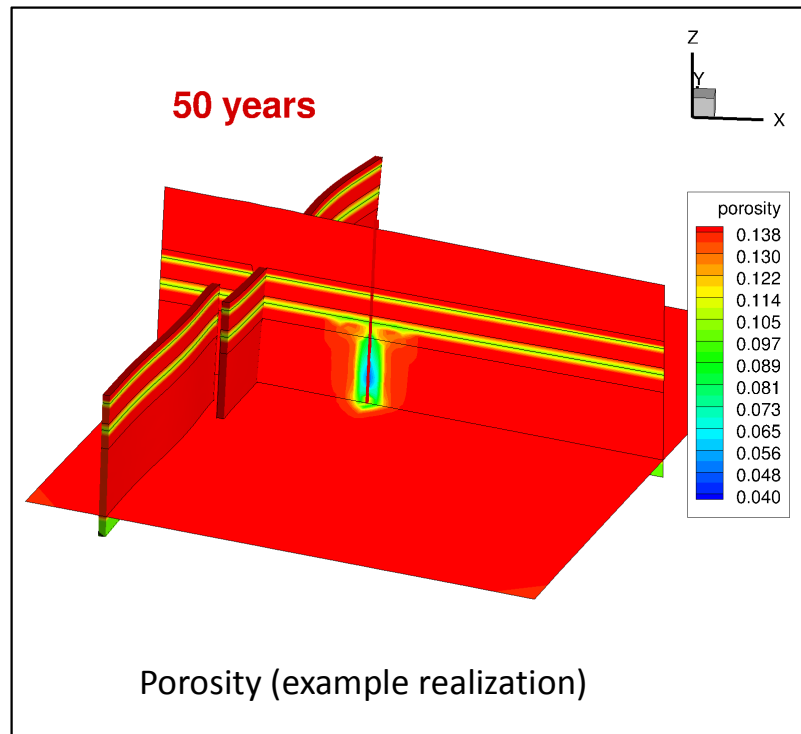
$$\frac{K}{K_o} = \left(\frac{\phi}{\phi_o}\right)^b$$

greatly increases required computational effort. Current research is focusing on using an emulator (PSUADE) to replace the functionality of a full numerical reactive transport model (following training) to improve computational efficiency and permit parameter sensitivity assessments.

Progress and Accomplishments: (3) Reactive Transport Modeling



Progress and Accomplishments: (3) Reactive Transport Modeling



Multiple reactive transport realizations (~hours of CPU time per realization) are required to generate response surfaces (i.e., training) for emulator. *Work in progress.*

Plan for Upcoming Research Year

- ▣ Research: apply statistical methods (e.g., Bayesian approaches) enabled by emulation and semi-analytical models to assess ...
 - Maximum fluid pressure on faults (fault reactivation risk)
 - Breakthrough of CO₂ to faults (leak risk)
 - Effects of uncertain operational inputs: injection rate, injection time, well perforation
 - Effects of initial heterogeneous porosity/permeability inputs: variance, horizontal and vertical correlation lengths
- ▣ Applications
 - Apply emulation and semi-analytical approaches to data from other U.S. and Chinese sites
 - Extension to CCS-EOR systems
- ▣ Effort
 - 0.5 FTE

5.3 Publications

The following abstract was published in Energy Procedia, which is the proceedings of the International Conference on Greenhouse Gas Technologies, held in Kyoto, Japan, November 18, 2012 through November 22, 2012. The abstract accompanies the poster presented above.

Walt McNab, John Rupp, Kevin Ellett, Jeff Wagoner, Simulating CO₂ Injection and Storage with Limited Site Data: the Utility of a Variably Complex Modeling Approach, Energy Procedia, Volume 37, 2013, Pages 3842-3849, ISSN 1876-6102, <http://dx.doi.org/10.1016/j.egypro.2013.06.281>.

A semi-analytical model for simulating injection of an immiscible fluid into a water-filled reservoir is developed which approximates the effects of horizontal injection wells, impermeable fault segments, and permeability anisotropy on phase saturation and fluid pressure. The modeling approach is based upon (1) an analytic element model for single-phase flow associated with specified flux, specified pressure, and impermeable line-segment elements within a reservoir of uniform thickness and porosity, (2) an analytical solution to the one-dimensional Buckley-Leverett equation for immiscible displacement of one fluid by another in porous media, subject to relative permeability functions dependent on fluid saturation, and (3) mapping of the Buckley-Leverett solution onto the two-dimensional flow field using particle tracking. Correction of the computed single-phase pressure distribution behind the fluid displacement front for two-phase flow is accomplished using a heuristic model. Application of the model to a proposed geological CO₂ storage system, characterized by an injection zone that is proximally cut by extensions of a regional fault system, include assessments of the impact of permeability, anisotropy, and other reservoir characteristics on fluid pressure distributions (and, by extension, the potential for induced seismicity resulting from a reduction in effective stress).

5.4 US-China ACTC Research Overview

The following section contains brief excerpts from the US-China ACTC Research Overview that pertain to Research Theme 6.

5.4.1 Theme 6 – Sequestration Capacity and Near-Term Opportunities

- 6.1 - Saline Formations at Basin Scale
- 6.2 - Geologic Storage and EOR
- 6.3 - Geologic Storage and ECBM
- 6.4 - Simulation and Modeling of Storage

Theme Leads – Li Xiaochun, Ren Xiangkun/Tim Carr, Ron Surdam, Phil Stauffer

- 6.1 – CAS (Li), WVU (Carr) and IGS (Rupp); SPIERCE (Zhou), UWYO (Surdam, Jiao)
- 6.2 – SPIERCE (Zhou), Yanchang (Gao) and UWYO (Jiao, Surdam)
- 6.3 – LLNL (Buschek)
- 6.4 – CUMT (Chu), LLNL (McNab) and LANL (Stauffer)

5.4.2 Accomplishments

- Assembled available information and data from Ordos Basin
- Inventoried the distribution of energy and CO₂ resources in Ordos Basin
- Delineated CO₂ sources and sinks in the Basin

- Explored the potential Ordos Basin analogs in Powder River, Greater Green River and Illinois Basins utilizing the latest performance and rock assessment simulation technology.

5.4.3 Plans

- Improve maps of major stationary CO₂ emission sources in Ordos Basin and potential storage/EOR sites
- Initiate pressure regime study to determine distribution of anomalous velocity regimes in Ordos Basin
- Continue comparative sedimentologic, stratigraphic, petrophysical, rock/fluid and comparative well log study of the Madison/Majiogou and Lance/Yanchang Formations
- Refine numerical simulations (performance and risk assessments with much improved databases) for CO₂ storage and EOR in Ordos Basin
- Build optimal strategy for EOR projects in Ordos Basin
- Develop commercial-scale geologic CO₂ storage/surge tank capabilities in the Ordos Basin.

5.5 CERC 2012-2013 Annual Report

The following section contains brief excerpts from the CERC 2012-2013 Annual Report that pertain to Research Theme 6.

5.5.1 CO₂ Sequestration U.S. Research Team Leaders

Tim Carr, West Virginia University

Ronald Surdam, University of Wyoming

Phil Stauffer, Los Alamos National Laboratory

Walt McNab, Lawrence Livermore National Laboratory

5.5.2 Research Objective

This theme's research is focused on estimating the CO₂ storage capacity of the Ordos Basin, China, and identifying near-term opportunities for geological CO₂ storage (carbon capture and storage [CCS] and carbon capture, utilization, and storage [CCUS]). This effort includes the following:

- Characterize targeted geological storage reservoirs in three dimensions, on both regional and site-specific scales, based on all available public geological, geophysical, geochemical, petrophysical, petrographic, and petroleum engineering data. This research is especially concerned with characterizing reservoir and seal heterogeneity, as well as the effects of heterogeneity on CO₂ injectivity and storage capacity assessments
- Develop the scientific, technological, and engineering framework required for CO₂ utilization in the Ordos Basin via enhanced oil recovery (EOR). The utilization strategy will include safe, permanent storage of large quantities of anthropogenic CO₂
- Develop simulation technology for CO₂ storage in saline formations
- Research and apply monitoring technology of CO₂ storage in saline formations
- Assess safety and risk of CO₂ storage in saline formations
- Understand system feedbacks, including the impacts of source locations on optimization of storage systems
- Conduct geological characterization

Through combined research on these issues and successful execution of demonstration projects, this effort will improve understanding, provide verification of key technologies for CO₂ storage in saline

formations, and provide the scientific evidence to implement large-scale CCS and CCUS in China and the United States.

The project has two primary objectives:

1. Build the scientific, technological, and engineering framework necessary for CO₂ utilization through EOR and the safe, permanent storage of commercial quantities of anthropogenic CO₂ in the Majiagou Limestone of the Ordos Basin, Shaanxi Province, China
2. Assess the safety and risk of CO₂ storage in saline formations

5.5.3 Technical Approach

In the near-term (2013), the team plans to accelerate data collection and move forward with work in the Ordos Basin (China), the Illinois Basin, and the Green River Basin (Rock Springs Uplift) in Wyoming. Both the United States and China are struggling to determine what data can be released publicly to facilitate collaboration that will allow use of the best algorithms from both China and the United States. Thus, an objective for 2013 is to generate regional-scale data from publicly available sources that can be shared between both countries. The team continues to monitor the progress of developments in the coal-to-liquid industry in the Ordos Basin.

Collaboration at the site scale will require application-dependent cooperation that may or may not involve direct sharing of sensitive data. Sharing executable algorithms will allow teams on either side to create results using the range of tools available to the U.S.-China Clean Energy Research Center (CERC). The team will continue to pursue opportunities to exchange personnel to increase productivity and joint understanding of algorithm implementation.

Both U.S. and Chinese teams will continue to develop models for specific sites in their own countries that will support the overall goals of the project without constraints. Specifically, using the University of Wyoming projects as analogs, the team proposes to work closely with research scientists from the Shaanxi Provincial Institute of Energy Resources and Chemical Engineering and Northwest University to assess the anthropogenic CO₂ resources and geological CO₂ storage capacity of the Ordos Basin.

The Yangchang Oil Company plans to initiate a CO₂ storage and CO₂-EOR project this summer. Company representatives plan to visit Wyoming in early summer to seek assistance with project design (e.g., reservoir heterogeneity characterization, structural and property modeling, injection and production simulation, economic evaluation). The joint project team has arranged a joint field trip in the Ordos Basin this summer to study the targeted storage reservoirs and potential sealing strata, and to observe cores in the Yanchang and North China Oil Company core repository. To assist the Yanchang Oil Company with its CO₂-EOR and storage demonstration projects, the team is planning a trip to work on the reservoir data at the Yanchang facility in order to continue to build structural and property models. Using these models, the team will perform numerical simulations for the targeted reservoir and storage site at facilities in Wyoming.

Detailed three-dimensional geological, structural, and property models will be constructed for the selected mature oil reservoir (i.e., targeted CO₂ flooding reservoir). Reservoir heterogeneity will be built

into these models using outcrop and core observations, well log analyses, seismic interpretations, and Wyoming analogs.

5.5.4 Recent Progress

In the last year, the partners from Northwest University, Shaanxi Provincial Institute of Energy Resources and Chemical Engineering, the Yanchang Petroleum Company, the North China Oil Company, the Institute of Rock and Soil Mechanics, China University of Mining and Technology, the University of Wyoming, Lawrence Livermore National Laboratory, Los Alamos National Laboratory, the Indiana Geological Survey, and West Virginia University have accomplished the following tasks:

- Assembled a large set of information regarding the geologic, petrophysical structural/stratigraphic frameworks of the Ordos Basin, Rock Springs Uplift, and Illinois Basin
- Inventoried the distribution of fossil energy and anthropogenic CO₂ resources in the Ordos Basin
- Delineated CO₂ sources and sinks in the Illinois Basin, the Ordos Basin, and sources for Wyoming
- Explored the potential of developing CCUS analogs between the Ordos Basin and the Powder River/Green River Basin and Illinois Basin using the latest screening criteria
- Published results from a numerical study of CO₂ injectivity, storage capacity, and leakage for the Rock Springs Uplift in Wyoming in the International Journal of Greenhouse Gas Control (Impact factor 5, Figure 2)
- Published results from an analysis of the impacts of CO₂ source variability on storage costs in Applied Energy (Impact factor 5)
- Published a methodology for regional-scale system analysis using data from the southeast United States in Energy & Environmental Science (Impact factor 9.5, Figure 3); methodology adapted partially from National Risk Assessment Partnership (NRAP) and applied to the Gibson site to emulate multiphase flow and reactive transport
- Developed site prioritization methods and ranked saline storage reservoirs
- Leveraged collaboration between the Yangchang Oil Company and the Theme 6 team to initiate design, construction, and injection at a pilot CO₂-EOR project in the Ordos Basin

5.5.5 Expected Outcomes

The significant opportunity for storage and utilization of CO₂ in the Ordos Basin in China complements opportunities that are being explored in basins in the United States, such as in Wyoming and Illinois. The research team is looking at the Ordos Basin in parallel to this research.

The lessons learned will be invaluable to CCS projects, particularly in Rocky Mountain basins; the Majiagou Limestone and Ordos Basin are very similar to the Paleozoic Madison Limestone and the Powder River Basin of Wyoming and Montana.

This work ultimately improves global understanding of how to safely and effectively store CO₂ in saline formations or to use the CO₂ for EOR.

The most important outcomes at the end of Year 5 are expected as follows:

- Jointly developed structural, property, and numerical models (including the heterogeneity of the reservoir/seal system) for the highest-priority geological CO₂ storage reservoirs and sites in the Ordos, Green River, and Illinois basins
- A detailed evaluation of all anthropogenic CO₂ sources and sinks in the Ordos, Green River, and Illinois basins
- Initial optimization strategies for pipeline networks in the same basins
- A demonstration project, developed in cooperation with Theme 6 partners, to evaluate the potential of integrated geological CO₂ storage with EOR using CO₂ flooding